Correlation between dissolved ^{4}He concentration and ^{36}Cl in groundwater at Äspö, Sweden

Yasunori Mahara*[a], Takuma Hasegawa[b], Kimio Miyakawa[b] and Tomoko Ohta[a]

[a]Research Reactor Institute, Kyoto University, Kumatori, Osaka 590-0494, Japan

[b]Civil Engineering Laboratory, Central Research Institute of Electric Power Industry, Abiko, Chiba 270-1194, Japan

* Author to whom correspondence should be addressed: Tel.:+81-724-51-2462, Fax: +81-724-51-2636, E-mail address: mahara@HL.rri.kyoto-u.ac.jp

Abstract Tunnel excavation at Äspö Island, Sweden, has caused severe groundwater disturbance, gradually extending deeper into the tunnel as present-day Baltic seawater intrudes through fractures connecting to the surface. However, the paleo-hydrogeochemical conditions have remained in the deep highly saline waters that have avoided mixing. A correlation has been observed between dissolved ^{4}He concentration and chloride ion concentration, measured every two years from 1995 to 2001 at Äspö. Groundwater mixing conditions can be examined by the correlations between 1/Cl, ^{36}Cl/Cl, and tritium concentrations. Subsurface production is responsible for the majority of the ^{36}Cl and excess dissolved ^{4}He of interstitial groundwater in fractures. The secular equilibrium ratio of ^{36}Cl/Cl in rock was theoretically estimated to be $(5.05 \pm 0.82) \times 10^{-14}$ based on the neutron flux intensity, a value comparable to the measured ^{36}Cl/Cl ratio in rock and groundwater. The degassing crustal ^{4}He flux was estimated to be $2.9 \times 10^{-8} \sim 1.3 \times 10^{-6}$ (ccSTP/cm^{2}y) using the HTO diffusion coefficient for the Äspö diorite. The ^{4}He accumulation rate ranges from 6.8×10^{-10} (for the *in situ* accumulation rate) to 7.0×10^{-9} (ccSTP/(g_{water}·y) considering both ^{4}He *in situ* production and the degassing flux, assuming ^{4}He is accumulated constantly in groundwater. By comparing the subsurface ^{36}Cl increase with ^{4}He concentrations in groundwater, the ^{4}He accumulation rate was determined from data for groundwater arriving at the secular equilibrium of ^{36}Cl/Cl. The ^{4}He accumulation rate was found to be $(1.83 \pm 0.72) \times 10^{-8}$ ccSTP/(g_{water}·y) without determining the magnitude of degassing ^{4}He flux.

Keywords: Groundwater mixing, excavation, ^{36}Cl/Cl ratio, subsurface production, secular equilibrium, excess ^{4}He, crustal ^{4}He flux

1. INTRODUCTION

Dissolved ^{4}He can be used to estimate groundwater residence time if the ^{4}He accumulation rate can be determined and is constant (Lehmann et al., 1993). In a pioneering study, Marine (1979) predicted groundwater flow velocity and residence time using only the *in situ* ^{4}He production rate. The results overestimated the residence time because the addition of ^{4}He from external sources was neglected. The mechanism of ^{4}He accumulation in groundwater is complex, and it has been variously discussed in terms of sources and accumulation processes. Some researchers have considered the crustal ^{4}He flux to be an external source for ^{4}He in flowing groundwater (Heaton, 1981; O'Nions and Oxburgh, 1983; Torgersen and Clarke, 1985; Martel et al., 1989; Stute et al., 1992; Marty et al., 1993; Ballentine et al., 2002), while others have argued that a sufficient concentration can be supplied from accumulated and produced ^{4}He in aquifer minerals (Tolstikhin et al., 1996; Solomon et al., 1996).

Ballentine et al. (2002) stated that a very long groundwater residence time cannot be determined from the ^{4}He flux from the crust into aquifers because regional ^{4}He accumulation rates vary greatly. Furthermore, the magnitude of the ^{4}He crustal flux has not been directly measured, but has only been indirectly estimated from the vertical ^{4}He profile using the ^{4}He diffusion coefficient in water and a suitable tortuosity parameter for rock (Osenbrück et al., 1998; Ballentine et al., 2002; Mahara and Igarashi, 2003). On the other hand, Andrews and Lee (1979) estimated a groundwater residence time of up to 30,000 years for the Bunter Sandstone in England using excess ^{4}He concentrations calibrated by ^{14}C ages. Lehmann et al. (2003) estimated the ^{4}He accumulation rate using only four groundwater samples, collected in the Great Artesian Basin of Australia, which were dated to more than 500 ka and calibrated using ^{81}Kr ages. However, these latter

authors calibrated the ^{4}He accumulation rate using cosmogenic radionuclides only, assuming constant ^{4}He accumulation.

Lippmann et al. (2003) also estimated the residence time of very old (1~168 Ma) groundwater in several deep gold mines in South Africa using ^{4}He, ^{40}Ar, ^{134}Xe and ^{136}Xe accumulation models, which consisted of *in situ* production and *in situ* production plus crustal flux. It was concluded that the *in situ* production model produced better estimations for the study basin than did the *in situ* production plus crustal flux model.

In this study, we discuss the correlation among dissolved ^{4}He concentration, chloride ion concentration and ^{36}Cl/Cl ratio under dramatic disturbances in groundwater caused by tunnel excavation. We try to reconstruct the correlation between dissolved ^{4}He concentration and the secular ^{36}Cl/Cl ratio using groundwater data that avoided severe mixing for the estimation of ^{4}He accumulation rate.

2. STUDY AREA AND GEOHYDROLOGICAL SETTING

The study area was the spiral tunnel of the Äspö Hard Rock Laboratory (HRL) constructed beneath Äspö Island, which is located about 400 km south of Stockholm on the eastern (Baltic Sea-facing) side of Sweden (Fig. 1). The tunnel was constructed between 1991 and 1995. Its total length is 3600 m, and its maximum depth is 460 m below sea level. Äspö Island itself is composed of Precambrian basement rock dated between 1.76 and 1.84 billion years by the U–Pb method (Stanfors et al., 1999). Major outcropping rocks are Småland granite and Äspö diorite, which are highly fractured and saturated. The Äspö site is characterized by swarms of fractures forming major fracture zones (Stanfors et al., 1999) which control the groundwater flow through the site.

Determination of the origin of groundwater is important for estimating residence

time and mixing among various end members. Although Laaksoharju et al. (1999) described the effects of prolonged water–rock interaction at Äspö, Louvat et al. (1999) estimated the addition of chlorine from rock to groundwater to be small. By comparing the changes in the Cl^-/Br^- ratios (e.g. the evolution indicator $\log(Cl^-/Br^-)$: 2.24 for KA2862A, 2.08 ~ 2.16 for KAS03, 2.08 ~ 2.17 for Lax-02, 2.59 for present-day Baltic seawater, and 2.46 for ocean water) in the evolution process of sea water and quoting Savoye's (1998) chlorine mass balance between dissolution from granite and salinity of deep groundwater, it was concluded that the origin of chlorine in these highly saline water was marine. Consequently, Louvant et al. predicted that the chlorine in the Äspö groundwater was supplied from marine derived water intruded into the Baltic shield at a time too ancient to estimate by the ^{36}Cl secular equilibrium method.

Quoting from Laaksoharju et al. (1999), present-day groundwater on the island is the result of mixing of five different end members: glacial meltwater, meteoric water, Baltic seawater, altered marine Baltic seawater, and brine. "Brine", with a very high chloride concentration (47000 mg/L) and thought to be extremely old, is found at the deepest location of a borehole at Laxemar (Lax-02, Fig. 1), located on the opposite shore of Äspö Island from the HRL tunnel. "Glacial meltwater" is cold-climate recharge, based on stable isotope values, and is 31,365 years old as determined by ^{14}C dating ($[Cl^-]$, 0.5 mg/L). "Baltic seawater" refers to the modern Baltic seawater ($[Cl^-]$, 3760 mg/L and 42 TU measured in 1992), while "altered marine Baltic seawater" ($[Cl^-]$, 4490 mg/L) is Baltic seawater affected by bacterial sulfate reduction, and is found within marine sediments. "Meteoric water" is non-saline water (chloride concentration, 5 mg/L), the tritium concentration in which was 59 TU measured in 1991.

Cyclic glacial activity in the study area has influenced long-term chemical

conditions for more than 1 million years. Although a dramatic local drawdown of the groundwater table (of approximately 80 m) has occurred in the past 15 years, due to the tunnel excavation as opposed to long-term natural events such as cyclic glaciation, hydrogeochemical changes in groundwater have been greater than could be caused by water–rock interactions. Therefore, mixing is an important factor for evaluating the chemical composition of groundwater under conditions of dramatic, local turbulent flow in an area where there has been significant regional and local fracturing.

Fractures and fracture zones are also critical because these control groundwater flow through Äspö Island (Laaksoharju et al., 1999). Based on detailed hydrogeological investigations (Stanfors et al., 1999), the water-bearing fracture zones are characterized by high hydraulic conductivity (in excess of 1×10^{-3} m/s). And, according to Mahara et al. (2001), the 17 major fracture zones probably control the dynamic flow via which present-day Baltic seawater and meteoric water intrude or mix with groundwater of different origins. Significant change in dissolved substance concentration in the short term is mainly controlled by dramatic changes in a geo-hydraulic condition. Stability of the groundwater chemistry depends on the extent of connectivity in the fracture network and the magnitude of the groundwater gradient, although some local dramatic changes in the groundwater environment have occurred through major fracture zones.

3. GROUNDWATER AND ROCK SAMPLING

At the Äspö site, major boreholes (HA and KA series) drilled in the tunnel were packed off at each fractured section. In order to monitor the effect of excavation on groundwater flow, groundwater hydraulic pressure has been continuously and automatically measured at each packed-off section since tunnel construction began. The

hydraulic pressure decreased by approximately 0.3 MPa between 1995 and 2001. The average difference from static hydraulic pressure since tunnel construction began in 1991 was approximately 0.6 MPa. The rate of decrease depends on the depths and locations of the boreholes. In general, the decrease in hydraulic pressure in shallow boreholes (e.g., HA1327B, KA2162B) has been greater than that in deep boreholes (e.g., KA2858A, KA3510A).

Groundwater samples were collected from the packed-off sections of the 13 boreholes in the tunnel every second year from 1995 to 2001 (Fig. 2) and, where possible, from other boreholes for reference. The groundwater samples were carefully collected to prevent degassing due to a reduction in water pressure and contamination by atmospheric air. A sampling head arrangement with control valves was used to maintain a hydraulic pressure of up to 25 MPa. The water pressure in the section was first gauged, and then an annealed copper tube, which had the sampling head arrangement opposite the opening, was connected to Teflon tubing coming out of the borehole. The copper tube was used to maintain the same pressure as that inside the packed-off borehole section while groundwater was drained directly from the isolated borehole section. Monitoring of the pressure gauge of the sampling head arrangement during sampling was conducted to ensure that the hydraulic pressure of the packed-off sections of the boreholes had been maintained throughout. After the pressure valve was opened, the borehole was purged of approximately three times the volume of groundwater in the isolated section while field parameters (electrical conductivity, pH, redox potential, dissolved oxygen content, and water temperature) were measured. Once there had been sufficient flushing to eliminate air bubbles from the inside wall of the copper tube, as visually confirmed by viewing the wall through the sampling head arrangement’s observation window, approximately 15 ml

of groundwater was pinched off in the annealed copper tube. This would be used for the analysis of dissolved noble gases.

One liter of groundwater was used for the analyses of the $^{36}Cl/Cl$ ratio and tritium, stable isotope and dissolved anion and cation concentrations. An attempt was also made to measure the ^{14}C concentration of high-salinity water samples (from boreholes SA2718A, KA2858A, KA2862A, and KA3010A) without detecting tritium. However, insufficient usable precipitation was collected from a 5-L groundwater sample; $SrCO_3$ was not visibly precipitated due to very low concentrations of bicarbonate ions (HCO_3^-) and pH values of 6.33 to 8.2 during the sampling time.

Six rock samples, approximately 15 to 20 cm long, were cut from the stored drill cores collected at KA2862A, KA3010A, KA3067A, KA3105A, KA3385A, and KA3510A. These included the section from which the groundwater samples were collected. These rock samples were used to estimate the intensity of the *in situ* neutron flux and subsurface ^{36}Cl production rate. Each rock sample was pulverized using an iron ball mill, and only rock powder that would pass through a 100-mesh sieve was retained. The powder was then repeatedly washed using super-pure distilled water, taking care to avoid AgCl precipitation originating from the residual saline water in rock mass micro-fractures. The powder was dried at room temperature in a clean room.

The analytical methods employed for determining the dissolved ^4He and tritium concentration and $^{36}Cl/Cl$ ratios in groundwater, and U and Th content in rock, are described in the Appendix.

4. RESULTS AND DISCUSSION

Noble gas, chloride, ^{36}Cl, and tritium concentrations for the collected groundwater

samples are presented in Table 1. Some groundwater samples had high excess Ne values; whether the mechanisms of partitioning were artificial or natural is not clear. The original, non-corrected data are used in the following discussion, since the concentrations of the heavier noble gases (i.e., Ar, Kr and Xe) could not be determined because of missing preparation. The $^{40}Ar/^{36}Ar$ ratio was measured, however, to confirm its increase in older groundwater (Davis and Bentley,1982; Rauber et al., 1991)**.**

4.1 Correlation between dissolved ^{4}He concentration and chloride concentration

The dissolved ^{4}He concentration increases as the groundwater sampling depth increases at the Äspö site (Fig. 3), although the rate of increase is not linear. In particular, the dissolved ^{4}He concentration varied greatly at –350 to –425 m depth, the result of intrusion directly into this deep location through fractures connecting to the surface zone by either shallow groundwater and/or modern Baltic seawater with low ^{4}He concentrations (Mahara et al., 2001). The ^{4}He concentration gradually decreased with an increase in time elapsed since the tunnel excavation, except in certain deep wells. The change in dissolved ^{4}He concentration from 1995 to 2001 can be attributed to the mixing of intruded modern Baltic seawater with the groundwater or of deep glacial brine that rose as a result of the deep turbulence caused by tunnel excavation.

Excavation in the deepest area of the site had just been completed in 1995, so the distribution of the ^{4}He concentrations observed in 1995 might closely reflect the virgin distribution before tunnel excavation. The correlation between the ^{4}He concentration (cm^3STP/m^3) in 1995 and sampling depth is expressed by the following exponential function:

$$^{4}He = 4.26\times10^{-5}\cdot\exp(-0.016\times z) \qquad (r^2 = 0.92) \qquad (1)$$

where z is the depth (m) from the ground surface to the sampling depth in the sampling well and has a negative value.

The dissolved ^{4}He concentration, which we can consider as a proxy for the sampling depth of groundwater, does not constantly increase with the chloride ion concentration; instead the relationship is a sigmoidal curve (Fig. 4). These disturbances in the ^{4}He concentration appear to be caused by the rise of deep saline groundwater, considered to be glacial brine (Laaksoharju et al., 1999), as a consequence of the complex water circulation that occurred during the tunnel excavation process. The relationship between the dissolved ^{4}He concentration and chloride ion concentration observed in 1995 probably reflects the original distribution, before tunnel excavation, in consideration of the low level of disturbance in the ^{4}He concentration in the high salinity zone (Fig. 4).

4.2 Origin of ^{36}Cl and estimation of the equilibrium ratio of $^{36}Cl/Cl$ in groundwater and the Äspö granite

At the Äspö site, the increase in $^{36}Cl/Cl$ ratio in the groundwater showed a strong positive correlation with the increase in the chloride concentration (Fig. 5). Figure 5 also shows the relationships between the $^{36}Cl/Cl$ ratio and chloride concentrations of Japanese and European commercial mineral waters, which mainly contain cosmogenic and/or bomb pulse ^{36}Cl, from around the world, and of ocean water collected from the Japan Sea (Mahara et al., 2004).

Consider two cases of simple mixing: commercial mineral water (Cl^-, 10 mg/L; $^{36}Cl/Cl$, 1×10^{-13}) with Japan Sea ocean water (Cl^-, 18000 mg/L; $^{36}Cl/Cl$, 3×10^{-16}) and with present-day Baltic seawater (Cl^-, 3760 mg/L; $^{36}Cl/Cl$, 1.8×10^{-15}), respectively. If all ^{36}Cl atoms in the water are cosmogenic, then the mixing lines showing the relationship

between the $^{36}Cl/Cl$ ratio and chloride concentration in the water are described by the formula $^{36}Cl/Cl = 1 \times 10^{-12}/Cl^- + 2.4 \times 10^{-16}$ for the ocean water and $^{36}Cl/Cl = 9.85 \times 10^{-13}/Cl^- + 1.53 \times 10^{-15}$ for present-day Baltic seawater (Fig. 5). However, the Äspö groundwater samples do not lie on either mixing line, indicating that the ^{36}Cl contained in groundwater at the Äspö site has a different origin from that of present-day Baltic seawater, ocean water, and commercial mineral waters.

According to Andrews et al. (1986), the maximum amount of excess ^{36}Cl atoms available via fallout from the bomb pulse is 1.4×10^9 n/L. If this was input into modern Baltic seawater, the apparent $^{36}Cl/Cl$ ratio would reach 2.19×10^{-14}. However, the observed $^{36}Cl/Cl$ ratio was only $(1.8 \pm 1.8) \times 10^{-15}$. Furthermore, if 1.4×10^9 n/L of excess ^{36}Cl atoms from the bomb pulse was added to shallow groundwater with the lowest chloride ion concentration of 4.51–42.02 meq/L at well KR0013B, the apparent $^{36}Cl/Cl$ ratio would range from 5.53×10^{-14} to 5.16×10^{-13}. In fact, however, the ratio changed only from a minimum of $(4.7 \pm 1.2) \times 10^{-15}$ in 1995 to a maximum of $(2.40 \pm 0.4) \times 10^{-14}$ in 1997. In other words, the contribution of airborne ^{36}Cl atoms from the bomb pulse or cosmic ray irradiation can be ignored in both shallow and deep groundwater.

In water samples with chloride concentrations of 5000 to 8000 mg/L, the $^{36}Cl/Cl$ ratio increased linearly from 1.8×10^{-15} to 4.0×10^{-14} as the number of ^{36}Cl atoms per liter of groundwater increased (Fig. 6). In samples with chloride concentrations above 10000 mg/L (Field “A” in Fig.6), the ratios were randomly distributed from 4.0×10^{-14} to 5.7×10^{-14} and were no longer linearly correlated with the number of ^{36}Cl atoms; instead, the ratios were closer to those of the brine samples from the Lax-02 borehole. This finding also indicates that ^{36}Cl was produced *in situ* in the subsurface and that the ratio had already reached secular equilibrium in groundwater with chloride concentrations greater

than 10000 mg/L, provided that most of chlorine originated in the intrusion of ancient seawater into the Baltic Shield as suggested by Louvant et al. (1999) and Savoye (1998).

To confirm the equilibrium ratio of ^{36}Cl/Cl in granite, we measured the ^{36}Cl/Cl ratios of six rock-matrix samples collected at KA2862A, KA3010A, KA3067A, KA3105A, KA3385A, and KA3510A. Since the Äspö granite is very old, if ^{36}Cl is generated in the rock then the ^{36}Cl/Cl ratios in its matrix should have reached secular equilibrium. The ^{36}Cl/Cl ratios measured in the rock matrix samples were $(5.10 \pm 0.60) \times 10^{-14}$ at KA2862A; $(8.60 \pm 0.60) \times 10^{-14}$ at KA3010A; $(9.70 \pm 0.80) \times 10^{-14}$ at KA3067A; $(1.52 \pm 0.54) \times 10^{-14}$ at KA3105A; $(1.27 \pm 0.42) \times 10^{-14}$ at KA3385A; and $(2.06 \pm 0.22) \times 10^{-14}$ at KA3510A. The measured ratios varied greatly among the six rock samples, perhaps because of the different rock types and the heterogeneous distribution of U and Th in the very small rock pieces sampled. The ^{36}Cl/Cl ratio in rock depends on the distribution and density of fissures and microfractures, where these neutron sources are concentrated (Moran et al., 1995). Trace elements, which absorb neutrons, also have a heterogeneous distribution in small rock pieces.

The secular equilibrium ratio can be theoretically calculated from the intensity of the estimated neutron flux in a rock matrix (Feige et al., 1968; Andrews et al., 1986) as follows:

$$^{36}Cl = \sigma \cdot \Phi \cdot {}^{35}Cl \cdot (1 - e^{-\lambda_{36} \cdot t}) / \lambda_{36} \qquad (2)$$

$$Cl = 1.7 \times 10^{22} \cdot \rho_{rock} \cdot [Cl] \qquad (3)$$

$$\left(\frac{^{36}Cl}{Cl} \right)_t = 4.55 \times 10^{-10} \cdot \Phi \cdot (1 - e^{-\lambda_{36} \cdot t}) \qquad (4)$$

where σ is the cross section for the neutron capture of ^{35}Cl (44 barns); Φ is the neutron flux produced by spontaneous fission and the (α,n) reaction induced by α particles

emitted from U and Th in the rock; Cl and ^{35}Cl are the total numbers of target nuclide atoms of $^{35+37}$Cl and ^{35}Cl in the rock, respectively, calculated from the chloride concentration ([Cl], ppm per 1 g of rock), a relative ^{35}Cl abundance of 0.758, and rock density ρ_{rock}; λ_{36} is the decay constant of ^{36}Cl (7.30×10^{-14} s). Using the measured concentrations of U, Th, and light and trace elements in Äspö granite, the neutron flux intensity was estimated to be $(1.11 \pm 0.18) \times 10^{-4}$ n cm^{-2}s^{-1}.

The average ^{36}Cl/Cl secular equilibrium ratio was subsequently calculated to be $(5.05 \pm 0.82) \times 10^{-14}$, whereas the average measured ratio in the six rock samples examined was $(4.71 \pm 3.72) \times 10^{-14}$. Furthermore, the measured ^{36}Cl/Cl ratios of seven groundwater samples that had high chloride concentrations (more than 10000 mg/L) averaged $(4.94 \pm 0.19) \times 10^{-14}$. These three secular equilibrium ratios, which were obtained by different methods, are consistent within approximately 10%. Consequently, we can accept $(5.05 \pm 0.82) \times 10^{-14}$ as the ^{36}Cl/Cl secular equilibrium ratio for the Äspö granite.

4.3 Groundwater mixing caused by intrusion of present-day Baltic seawater

According to Banwart et al. (1994), Laaksoharju et al. (1999), and Mahara et al. (2001), tunnel excavation caused large-scale intrusion of modern Baltic seawater, which penetrated deeply via fractures into the bedrock. To characterize the effect this intrusion would have on Äspö groundwater, mixing between modern Baltic seawater (Cl^-, 3760 mg/L; ^{36}Cl/Cl, 1×10^{-15}) and waters with different salinities and different ^{36}Cl/Cl ratios was examined. For the latter, waters with a Cl^- concentration of 47000 mg/L and a ^{36}Cl/Cl ratio of 5.05×10^{-14} were considered to be brine; those with respective values of 16000

mg/L and 5.05×10^{-14} to be high-salinity water, found in the deepest part of the Äspö site; those with values of 10000 mg/L and 5.05×10^{-14} to be high-salinity glacial brine; those with values of 5000 mg/L and 5.05×10^{-14} to be low-salinity glacial brine; those with values of 1000 mg/L and 5.05×10^{-14} to be relatively high salinity, shallow groundwater; those with values of 100 mg/L and 1×10^{-13} to be relatively low salinity, shallow groundwater; and those with values of 10 mg/L and 1×10^{-13} to be meteoric water. Figure 7 shows the relationships between 1/Cl and $^{36}Cl/Cl$ ratios that would result from the mixing of present-day Baltic seawater with such waters.

Most groundwater samples with $^{36}Cl/Cl$ ratios greater than 2.5×10^{-14} are distributed in the mixing zone between present-day Baltic seawater and water with chloride concentrations higher than 10000 mg/L; tritium is not detectable in these waters. On the other hand, water with relatively low $^{36}Cl/Cl$ ratios, in which tritium is detectable, is distributed in the mixing zone between modern Baltic seawater and low-salinity water, with chloride concentrations of less than 5000 mg/L. When groundwater was mixed with present-day Baltic seawater (Fig. 7), the mixing indicator employed was the detection limit of tritium (0.3 TU, see Appendix). Tritium concentrations in seawater and in the shallow groundwater surrounding the Äspö site have remained relatively high. The origin of the tritium is global fallout from nuclear weapons testing before the early 1960s and other artificial sources such as release from nuclear facilities. Although it is not clear whether artificial contributions have maintained tritium at a relatively high level in present-day Baltic seawater, there are nuclear power plants and spent-fuel storage facilities near the Äspö site.

Since Baltic seawater in 1992 and shallow groundwater in 1991 had tritium concentrations of 42 TU and 60 TU, respectively (Banwart et al., 1994), in 2001 the

tritium detection limit in a mixture was equivalent to the inclusion of approximately 1.14% of present-day Baltic seawater. Therefore, if the groundwater has mixed homologously with modern Baltic seawater, it should be possible to detect tritium in all of the samples. However, in several water samples, tritium was not detected (Fig. 7, solid squares). Most groundwaters lacking tritium are aligned with mixing lines between present-day Baltic seawater and brine or high-salinity water with more than 10000 mg/L of chloride. Although these waters, based on their location on the plot, contain at least 50% modern Baltic seawater, tritium was not detected in them. This finding is inconsistent with the relationship between the tritium detection limit and the mixing rate with modern Baltic seawater. This contradiction led us to infer that these waters at the time of sampling had not yet become mixed with modern Baltic seawater as a result of tunnel excavation.

Alternatively, mixing between ancient Baltic seawater (with maximum chloride concentrations of 8300 mg/L and a $^{36}Cl/Cl$ ratio of 1×10^{-15}) and water with various salinities and $^{36}Cl/Cl$ ratios was investigated (Fig. 8). Ancient Baltic seawater has a maximum salinity of about twice that of modern Baltic seawater (Ekman, 1953). The salinity (S) of ancient Baltic seawater, estimated as 10–15‰, was approximately converted to 5500–8300 mg/L of chloride ions using the equation $S = 1.80655 \times Cl$ (g/L) (Clesceri et al., 1989). Most of the samples from areas in which tritium was undetectable and with a salinity of more than 10000 mg/L were aligned with one of these mixing lines. Thus, the high-salinity groundwater samples that strayed greatly away from the mixing lines between present-day Baltic seawater (Fig. 7) possibly preserve ancient hydrogeochemical conditions produced by subsurface paleo-mixing at the Äspö site.

It can therefore be concluded that great changes in hydrogeochemical conditions were

caused by the dramatic drawdown of the water table resulting from tunnel excavation, but that at the time of sample collection several waters had not yet been affected by mixing with modern Baltic seawater. Moreover, we cannot exclude the possibility that some waters have preserved their ancient hydrogeochemical characteristics.

4.4 Estimated magnitude of the crustal degassing flux of ^{4}He and the ^{4}He accumulation rate in groundwater

The magnitude of the crustal degassing flux of ^{4}He was estimated using the following equation (Andrews, 1985):

$$J_{He} = 2G\sqrt{\frac{D_{He}T}{\pi}} \qquad (5)$$

where G is the production rate of He in rock (3.4×10^{-12} ccSTP/(cm^3.y)$_{rock}$), T is the age of the rock formation (1.8×10^9 years), and D_{He} is the ^{4}He diffusion coefficient in the granite matrix, where fractures and microfractures are assumed to be the main routes of ^{4}He transport.

Although a typical diffusion coefficient of dissolved ^{4}He has not yet been determined for Äspö granite, Holgersson et al. (1998) reported $(6.5–25) \times 10^{-14}$ m^2/s to be the diffusion coefficient of HTO (titrated water) in Äspö diorite, which is one of the typical granites at the Äspö site. However, ^{4}He transport in the crust might best be explained by using one ^{4}He diffusion coefficient for the matrix and another for the water-filled micropores, as in the wet-sponge model described by Andrews et al. (1989b). In the present case, a larger value for the diffusion coefficient for dissolved ^{4}He was used than found for HTO, because the diffusion of dissolved ^{4}He is greater than HTO. When the crustal ^{4}He flux was estimated using ^{4}He diffusion coefficients of 1×10^{-13} and $1 \times$

10^{-12} m^2/s, the ^4He flux ranged from 2.9×10^{-8} to 9.1×10^{-8} $cm^3(STP)\ cm^{-2}\ y^{-1}$ at the Äspö site.

The magnitude of the ^4He degassing flux (J_{He}) was also estimated, using the ^4He profile (Eq. 1 and Fig. 3), the ^4He diffusion coefficient values reported for the Äspö diorite, and Fick's analogous equation:

$$J_{He} = -D_{He} \cdot \frac{dHe}{dZ} \qquad (6)$$

The gradient of the ^4He concentration ($m^3STP \cdot m^{-3}_{water} \cdot m^{-1}$) was calculated using Eqs. (1) and (6) as $\frac{dHe}{dZ} = -6.8 \times 10^{-7} \cdot \exp(-0.016 \cdot Z)$. The magnitude of the ^4He degassing flux at a depth of Z = –400 m was predicted to be between 1.3×10^{-7} and 1.3×10^{-6} ($ccSTP/(cm^2\ y)$), using the two ^4He diffusion coefficients 1×10^{-13} and 1×10^{-12} $m^2 \cdot s^{-1}$, respectively.

The crustal ^4He fluxes estimated in these two different ways range from 2.9×10^{-8} to 1.3×10^{-6} ($ccSTP/cm^2\ y$). These are smaller (up to two orders of magnitude less) than the values of 3.3×10^{-6} $cm^3(STP)\ cm^{-2}y^{-1}$, reported by O'Nions and Oxburgh (1983) and used to explain the global atmospheric He budget (Torgersen, 1989), and the value of 3.6×10^{-6} $cm^3(STP)\ cm^{-2}y^{-1}$ for the Great Artesian Basin (GAB), estimated by Torgersen and Clarke (1985). However, these estimated ^4He flux results are comparable to other estimated degassing ^4He flux magnitudes from around the world: for example [$ccSTP/(cm^2\ y)$ in each case], 4.4×10^{-7} for the Paris Basin (Marty et al., 1993); 2.9×10^{-6} (Martel et al., 1989) and $(0.8–5.2) \times 10^{-7}$ (Stute et al., 1992) for the Great Hungarian Plain; $(2.3–3.0) \times 10^{-7}$ for the Molasse Basin in Austria (Andrews et al., 1985); 2.0×10^{-7} for the Morsieben Basin in Germany (Osenbrück et al., 1998); $(2.2–2.9) \times 10^{-6}$ for the Auob Sandstone Aquifer in Namibia (Heaton, 1984); $(2.8–3.1) \times 10^{-6}$ for northern Taiwan (Sano et al.,

1986); and 4.9×10^{-7} for the Rokkasho Basin in Japan (Mahara and Igarashi, 2003).

Groundwater residence times (T) can be calculated using the estimated ^{4}He degassing flux and Eq. (7), as per studies conducted by Torgersen and Clarke (1985), Stute et al. (1992), Osenbrück et al. (1998), and Lippmann et al. (2003):

$$T = \frac{He_{excess}}{\frac{J_{He}}{\rho_{water} \cdot \phi \cdot Z} + A} \qquad (7)$$

where He_{excess} is the excess ^{4}He concentration in groundwater (ccSTP/g_{water}), ρ_{water} is the density of the water (1.0 ~ 1.188 g/cm^3), φ is the porosity of the rock (0.005), Z is the sampling depth of the groundwater (400 m), and A is the *in situ* accumulation rate in pore water. Employing the density of brine water cited in Frape et al. (1984), which has a maximum chloride ion concentration of 168,000 mg/L in the Canadian Shield, it was estimated that the oldest groundwater residence time was approximately 4.3–25 million years at KA2862A in 1995.

Conversely, the ^{4}He accumulation rate can be calculated from the oldest residence time. The approximate accumulation rates were subsequently found to range from 1.2×10^{-9} to 7×10^{-9} (ccSTP/(g_{water} y)). These values are several times the average *in situ* ^{4}He accumulation rate of 6.76×10^{-10} (ccSTP/(g_{water} y)) in the Äspö granite and, furthermore, are significantly greater than the ^{4}He accumulation rate of 2.91×10^{-10} (ccSTP/(g_{water} y)) estimated for the GAB (Torgersen and Clarke, 1985). Nevertheless, the estimated crustal ^{4}He flux was small at the Äspö site, because the porosity of the local rock (0.5%) is very small compared with that (20–30%) in the aquifer of the GAB.

4.5 Reconstruction of the relationship between the dissolved ^{4}He concentration and

the ^{36}Cl/Cl ratio

Groundwater flows through fractures or fissures in the granite at the Äspö site. Most ^{36}Cl atoms in groundwater in granite fractures are produced *in situ* through neutron capture. Since thermal neutrons are absorbed in rock over a mean free path of approximately 50 cm, the stable chlorine atom ^{35}Cl is equally likely to be activated in interstitial water in fractures as in rock (Lehmann et al., 1997).

The ^{36}Cl/Cl ratio gradually reaches a constant level in relation to the increasing dissolved ^{4}He concentration in old groundwater, because the production of ^{36}Cl by neutron capture and its subsequent decay reach radioactive equilibrium, and the ^{36}Cl/Cl ratio approaches secular equilibrium. The ^{36}Cl/Cl ratio changes exponentially ($1 - \exp(-\lambda t)$), where λ is the decay constant and t is elapsed time. If we express elapsed time as the dissolved excess ^{4}He concentration, a strong correlation is observed between the increasing ^{36}Cl/Cl ratio and the ^{4}He concentration (Fig. 9).

The ^{36}Cl/Cl ratio increases dramatically as the dissolved ^{4}He concentration increases up to 0.01 ccSTP/g, but then it tends to level off when the ^{4}He concentration reaches 0.02 ccSTP/g as secular equilibrium conditions are attained(Fig. 9). If confirmation of both the edge point as the lower limit of the ^{36}Cl/Cl ratio at secular equilibrium and the starting point is possible, a theoretical growth curve of ^{36}Cl in relation to the dissolved ^{4}He concentration can be fitted. The starting point of this theoretical curve for the Äspö groundwater system can easily be set; surface seawater has a low ratio of ^{36}Cl/Cl (approximately 0) owing to great dilution by stable chlorine and low dissolved ^{4}He concentrations that are close to equilibrium with atmospheric ^{4}He in shallow seawater. However, if the linear correlation between radioactive decay and ^{4}He concentration has been kept after mixing, then the theoretical neutron activation curve

can be fitted.

Mixing is important for a dramatic change in ^{36}Cl and ^{4}He concentration in the very short term like a tunnel excavation. We examined the effect of simply mixing groundwater with tracers of different concentrations. When groundwater A ($^{36}Cl/Cl$ ratio, R_A; chloride concentration, Cl_A; ^{4}He content, He_A) mixes with groundwater B ($^{36}Cl/Cl$ ratio, R_B; chloride concentration, Cl_B; ^{4}He content, He_B), the ^{4}He concentration in the mixture maintains linearity to the elapsed time because ^{4}He is a stable element and its concentration is linearly related with time if ^{4}He accumulates at a constant rate. On the other hand, the $^{36}Cl/Cl$ ratio usually deviates from the exponential curve that is controlled by radioactive decay, as discussed by Park et al. (2002). However, if both groundwaters A and B have already reached secular equilibrium (i.e., $R_A = R_B$ = constant secular equilibrium ratio), the $^{36}Cl/Cl$ ratio in the resulting mixture does not change: that is, $R = \frac{m \cdot (R_A \cdot Cl_A) + n \cdot (R_B \cdot Cl_B)}{m \cdot Cl_A + n \cdot Cl_B}$, $m + n = 1$, $m \geq 0$ *and* $n \geq 0$. If R_A and R_B are the same secular equilibrium ratio, then R is equivalent to $R_A=R_B$. Thus, if two groundwaters in secular equilibrium with respect to the $^{36}Cl/Cl$ ratio are mixed, then the ratio should keep constant in relation to the ^{4}He concentration. In other words, the linear correlation between the radioactive decay and ^{4}He concentration should be retained after mixing.

The theoretical correlation curve fitted after omitting all data points where the groundwater does not fall within the secular equilibrium range owing to mixing is given in Fig. 10. The remaining data points correspond to the data collected at boreholes SA2718A, SA2743A, SA2783B, KA2858A, and KA2862A, where Mahara et al. (2001) confirmed that the groundwater was very old and increased in the $^{40}Ar/^{36}Ar$ ratio as compared to that of atmospheric Ar. These samples should show a linear correlation

between the dissolved ^{4}He concentration and the elapsed time with the constant secular equilibrium ^{36}Cl/Cl ratio even if groundwater mixing occurred because of the tunneling. However, the data relating to SA2783B was deleted from the data set, because SA2783B contains a small amount of tritium (1.69 ± 0.25 TU) indicating that it has recently been affected at least by a shallow groundwater intrusion.

In this analysis, the modern Baltic seawater was used as the starting point and sample KA2858A as the location of the lower limit of secular equilibrium for ^{36}Cl/Cl. The growth curve of the ^{36}Cl/Cl ratio (Fig. 10) is described by the following equation (r^2 = 0.96):

$$\left(\frac{^{36}Cl}{Cl}\right)_t = \left(\frac{^{36}Cl}{Cl}\right)_{eq} \times \{1 - \exp(-(126 \pm 49.7) \times He)\} \qquad (8)$$

where He is the dissolved excess ^{4}He concentration (ccSTP/g) in groundwater. $(^{36}Cl/Cl)_{eq}$ is the best fitted secular equilibrium ratio, (5.26 ± 0.24) × 10^{-14}, for the groundwater, which is a slightly lager than the value estimated in the section 4.2. Nevertheless, it is acceptable considering the inclusion of the measurement error in the ^{36}Cl/Cl ratio which is more than 10%.

From Fig. 10, the accumulation rate of ^{4}He is found to be (1.83 ± 0.72) × 10^{-8} ccSTP/(g_{water}·y). While this is approximately 27 times greater than the *in situ* production rate of ^{4}He, it is significantly smaller than 72 times greater found in the GAB (Torgersen and Clarke, 1985). Furthermore, this rate is two to ten times greater than that estimated from the simple ^{4}He diffusion model. Although there are still some data quality problems and more discussion is required to determine the edge point as the lower limit of the ^{36}Cl/Cl ratio at secular equilibrium in the sever groundwater mixing, it is proposed that this method can estimate the ^{4}He accumulation rate without prior determination of the

magnitude of ^{4}He degassing flux.

5. CONCLUSIONS

The study's major conclusions are as follows.

(1) Groundwater at the Äspö site has been disturbed and become mixed as a result of a great intrusion of present-day Baltic seawater caused by the tunnel excavation. Moreover, the disturbance increased at deep sites at each later observation due to a deep turbulent flow of groundwater with high density and high salinity generated by movement of modern Baltic seawater through the many fractures connecting the deep sites with the surface as a result of groundwater being pumped out of the tunnel. Although the variation in the dissolved ^{4}He concentration in high-salinity water changed with time elapsed since the tunnel excavation, the distribution of the ^{4}He concentration observed in 1995 is probably close to the original distribution before tunnel excavation, given that the tunnel first penetrated to deep locations in 1995 and because a good correlation between dissolved ^{4}He concentration and chloride concentration was observed in samples collected in 1995.

(2) The ^{36}Cl/Cl ratio increased linearly in relation to the number of ^{36}Cl atoms to 4×10^{-14} in Äspö groundwater samples with 5000–8000 mg/L of chloride. The ratio at chloride concentrations above 10000 mg/L, which was greater than 4×10^{-14} (the value estimated to be the secular ratio for brine at Laxemar), ceased to correlate with the number of ^{36}Cl atoms. This suggests that ^{36}Cl in the groundwater at Äspö is not cosmogenic, but was produced *in situ* through the neutron capture of ^{35}Cl atoms in interstitial water in the granite. The intensity of the neutron flux in the deep-rock environment was estimated to average $(1.11 \pm 0.18) \times 10^{-4}$ n $cm^{-2}.s^{-1}$. The secular

equilibrium ratio of $^{36}Cl/Cl$ in the rock was estimated to be $(5.05 \pm 0.82) \times 10^{-14}$.

(3) Groundwater mixed and unmixed conditions were distinguished by investigating the relationship between 1/Cl and $^{36}Cl/Cl$. Although tunnel excavation caused severe disturbance in groundwater because of deep intrusion of present-day Baltic seawater, some waters escaped mixing and have maintained their paleo-hydrogeochemical condition. These waters show evidence of mixing with ancient Baltic seawater, which had higher salinity than the modern Baltic seawater.

(4) The crustal degassing flux of ^{4}He was estimated to range from 2.9×10^{-8} to 1.3×10^{-6} (ccSTP/cm^2 y) by using two different methods. Although this is up to two orders of magnitude smaller than that estimated in the GAB, it is comparable to values estimated for other basins in the world. The ^{4}He accumulation rate ranged from 1.2×10^{-9} to 7×10^{-9} (ccSTP/(g_{water} y), though the ^{4}He diffusion coefficient for the Äspö granite still needs to be estimated accurately.

(5) In interstitial water and rock, the number of ^{36}Cl atoms increases over time owing to the constant neutron flux. If the concentration of dissolved ^{4}He also increases constantly with time, changes in the ^{4}He concentration can be used to represent elapsed time. Therefore, it is possible to determine the magnitude of the ^{4}He accumulation rate from the relationship between the increasing ^{4}He concentration and the increasing $^{36}Cl/Cl$ ratio. When two groundwaters, both at secular equilibrium with respect to the $^{36}Cl/Cl$ ratio, are mixed, the ratio ceases to change and the dissolved ^{4}He concentration maintains linearity to the elapsed time despite the severe disturbance caused by tunneling. The actual ^{4}He accumulation rate at the Äspö site was estimated to be $(1.83 \pm 0.72) \times 10^{-8}$ ccSTP/(g_{water}·y), using data from samples in which the $^{36}Cl/Cl$ ratio had reached secular equilibrium. This is approximately twenty seven

times the value estimated on the basis of *in situ* production (6.76×10^{-10} (ccSTP/(g_{water}·y)). Reasonable ^{4}He accumulation rates probably range from 6.76×10^{-10} to $(1.83 \pm 0.72) \times 10^{-8}$ ccSTP/(g_{water}·y) for the Äspö site, though the determination of the edge point as the lower limit of the ^{36}Cl/Cl ratio at secular equilibrium requires further work.

Acknowledgements: This work was part of the cooperative research between SKB and CRIEPI during the period from 1995 to 2002. I thank Dr. P. Wikberg (Swedish Nuclear Fuel and Waste Management Company) for arranging this fieldwork at Äspö HRL. I further thank Prof. L. K. Fifield (Australian National University), Dr. R. G. Cresswell (Commonwealth Scientific and Industrial Research Organization), and Prof. M. Suter and Dr. H. A. Synal (Swiss Federal Institute of Technology) for measuring ^{36}Cl in the Äspö groundwater, and Prof. D. Elmore (Purdue University) for measuring ^{36}Cl in rock matrixes using an accelerator mass spectrometer. At last, we thank Dr. Hunt and one anonymous reviewer for their critical comments on the manuscript.

Appendix: Analytical protocols

Tritium

Tritium concentrations were measured by counting beta rays after electrolytic enrichment (Japanese Science and Technology Agency, 1976). One liter of groundwater was reduced to about 40 ml by electrolysis using Ni/Fe electrodes. Forty milliliters of distillate and 60 ml of scintillation cocktail were mixed in a 100-ml Teflon vial. This mixture was analyzed for 1000 min using a low-background liquid-scintillation counter. The detection limit for this method is 0.3 TU.

U and Th in the rock

A sample of 0.5 g of pulverized rock powder was placed in a Teflon beaker and completely dissolved by adding concentrated HNO_3 and HF and heating on a hot plate. After subsequent addition of concentrated HNO_3 and $HClO_4$ to the resolved material, the mixture was again heated until $HClO_4$ fuming occurred. The re-resolved material was diluted with a small amount of weak HCl, and diluted further to 100 ml using super-pure distilled water. The U and Th concentrations were measured using inductively-coupled plasma mass spectrometry (ICP-MS) (Japanese Ministry of Education and Science, 2002).

Dissolved noble gases

Dissolved noble gases were separated from the water samples using 15 min of ultrasonic vibration in a stainless steel extraction line under high vacuum (1×10^{-6} mbr), after attaching the pinched-off annealed copper tube and removing one pinch-off using a reopening device. A liquid nitrogen cold trap removed the water vapor and condensable gases. Active gases were removed using two titanium-zirconium getters, one heated to 450 °C and the other at room temperature. The 1-cc gas sample was separated from the residual gas, which excluded active gases, and was isolated in a stainless steel ampoule bottle for measurement of argon isotopic ratios. Heavy noble gases (Ar, Kr, and Xe) in the residual gas in the extraction line were removed by two activated charcoal traps cooled in liquid nitrogen, and further cooled to 40 K using a cryogenic pump to remove residual argon and moisture.

The residual He and Ne mixture in the purification unit was fed into a VG-5400 mass

spectrometer (Micro Mass Ltd). First, the concentration of ^{4}He and the ^{20}Ne/^{4}He ratios were measured six times in 10 min. The mixture was then cooled to 22 K using a cryogenic pump to remove Ne, and gas fed back through the spectrometer to measure the ratio of ^{3}He to ^{4}He. This was repeatedly measured (at least 50 times) over approximately 60 min, with a standard deviation of 1σ at less than 1%. The precise values of the ^{4}He concentrations, ^{20}Ne/^{4}He ratios, and ^{3}He/^{4}He ratios were determined by comparison with two sets of standard air values measured under the same conditions before and after measuring the samples. This study assumed the ratio of ^{3}He/^{4}He in standard air to be 1.384×10^{-6} (Clarke et al., 1976). The ^{4}He concentrations, ^{3}He/^{4}He ratios, and ^{20}Ne/^{4}He ratios were determined with measurement errors of less than 0.5, 1, and 5%, respectively (described in detail in Sano et al., 1993). These errors, which do not include sampling errors from loss or contamination, were verified through the reproducibility of the ^{4}He concentration measurements in the standard air sample and the ratios of ^{3}He/^{4}He and ^{20}Ne/^{4}He dissolved in the distilled water samples, and by using 2.4×10^{-9} ccSTP and 7.2×10^{-9} ccSTP as system blanks for ^{4}He and ^{20}Ne, respectively. The average gas-stripping efficiency of the dissolved gases from the water samples was determined to be 97% by comparing the ^{4}He extracted from distilled water equilibrated with atmospheric air at 23ºC to the data in the literature (Weiss, 1971).

^{36}Cl/Cl ratio

Chloride was precipitated as AgCl in a clean room. The precipitate was purified by repeated re-dissolution in NH_4OH and re-precipitation (after the removal of sulfur as $BaSO_4$). All AgCl precipitation samples to be used in accelerator mass spectrometry (AMS) measurements were made following the standard procedures used at the

Australian National University (ANU) (Creswell, 2001). The $^{36}Cl/Cl$ ratios for the groundwater samples were measured using accelerator mass spectrometers located at ANU and at ETH in Zurich. Measurement of the $^{36}Cl/Cl$ ratio for the rock samples was performed using the accelerator mass spectrometer at the Prime Laboratory, Purdue University, West Lafayette, IN, USA, after chemical Cl separation as AgCl and purification of its precipitation from the rock matrix.

References

Andrews N. J., 1985. The isotopic composition of radiogenic helium and its use to study garoundwater movement in confined aquifers. Chem. Geol. 49, 339-351.

Andrews J. N. and Lee D. J., 1979. Inert gases in groundwater from the Bunter Sandstone of England as indicators of age and paleoclimatic trends, J. Hydrol. 41, 233-252.

Andrews J. N. Goldbrunner J. E., Darling W. G., Hooker P. J., Wilson G. B., Youngman M. J., Eichinger L., Rauert W., and Stichler W., 1985. A radiochemical, hydrochemical and dissolved gas study of groundwaters in the Molasses basin of Upper Austria. Earth Planet. Sci. Lett., 73, 317-332.

Andrews N. J., Fontes J.-Ch., Michelot J.-L. and Elmore D., 1986. In-situ neutron flux, ^{36}Cl production and groundwater evolution in crystalline rocks at Stripa, Sweden, Earth Planet. Sci. Lett. 77, 49-58.

Andrew J.N., Davis S.N., Fabryka-Martin J., Fontes J.-Ch., Lehmann B.E., Loosli H.H., Michelot J.-L., Moser H., Smith B. and Wolf M., 1989a. The in-situ production of radioisotopes in rock matrices with particular reference to the Stripa granite, Geochim. Cosmochim. Acta, 53,1803-1815.

Andrews N. J., Hussain N. and Youngman M. J., 1989b. Atmospheric and radiogenic gases in groundwaters from the Stripa granite, Geochim. Cosmochim. Acta, 53, 1831-1841.

Ballentine C. J., Burgess R. and Marty B., 2002. Tracing fluid origin, transport and interaction in the crust, in: Noble gases in Geochemistry and Cosmochemistry, Rev. Mineral 47, 539-614.

Banwart S., Gustafsson E., Laaksoharju M., Nilsson A.-Ch., Tullborg E.-L., and Wallin B., 1994. Large-scale intrusion of shallow water into a vertical fracture zone in crystalline bedrock: Initial hydrochemical perturbation during tunnel construction at the Hard Rock

Laboratory, southereastern Sweden, Wat. Resour. Res., 30, 1747-1763.

Bethke M. C. and Johnson M. T., 2002. Paradox groundwater age, Geology 30, 385-388.

Clarke W.B., Jenkins W. J. and Top Z., 1976. Determination of tritium by mass spectrometric measurement of ^{3}He, Jour. Applied Radiation Isotopes 27, 515-522.

Clesceri, L. S., Greenberg, A. E. and Trussell, R. R., 1989. *Standard Methods for the Examination of Water and Wastewater*, 17th edn. American Public Health Association, Washington, DC, USA.

Creswell R. G., 2001. Manual for groundwater sample preparation for ^{36}Cl analysis (version: March 1999) (private communication)

Davis N. S. and Bentley W. H, 1982. Dating groundwater: A short review, *In Nuclear and Chewmical Dating Techniques- Interpreting the environmental record*, *Currie A. Lloyd (ed.)*, Based on a symposium jointly sponsored by the Divisions of Nuclear and Technology, Geochemistry, and History of Chemistry at the 179th Meeting of the American Chemical Socity, Houston, Texas, March 24-25, 1980, pp.187-222.

Ekman S., 1953. Zoogeography of the Sea. Sidwick and Jackson. London. 417 pp.

Feige Y., Oltman B.G. and Kastner J., 1968. Production rates of neutrons in soils due to natural radioactivity, J. Geophys. Res. 73, 3135-3142.

Frape S.K, Fritz P. and McNutt R. H., 1984. Water-rock interaction and chemistry of groundwaters from the Canadian Shield, Geochim. Cosmochim. Acta, 48,1617-1627.

Heaton T. H. E., 1981. Dissolved gases: some applications to groundwater research, Trans. Geol. Soc. Afr. 84, 91-97.

Heaton T. H. E., 1984. Rate and sources of ^{4}He accumulation in groundwater. Hydrol. Sci. J., 29, 29-47.

Holgersson S., Albinsson Y., Engkvist I., Rochelle C. and Pierce J., 1998. Interaction of cement pore fluids with host rock and the effects on HTO, Na and Cs diffusion. Radiochim. Acta., 82, 197-203.

Japanese Science and Technology Agency, 1976. Analytical procedure for tritium. (in Japanese). Radiation Manegement Ser. 122. Japan Chem. Anal. Center, Sanno, Chiba, Japan.

Japanese Ministry of Education and Science, 2002. Analytical procedure for uranium (in Japanese). Radioactivity Measurement Ser. 14, pp.96., Japan Chem. Anal. Center, Sanyo, Chiba, Japan.

Laaksoharju M., Tullborg E.-L., Wikberg P., Wallin B. and Smellie J., 1999.

Hydrogeochemical conditions and evolution at the Äspö HRL, Sweden, Appl. Geochem. 14, 835-859.

Lehmann B. E., Davis S. N. and Fabryka-Martin J. T., 1993. Atmospheric and subsurface sources of stable and radioactive nuclides used for groundwater dating, Water Resour. Res. 29, 2027-2040.

Lehmann B. E., Love A., Purtschert R., Collon P., Loosli H. H., Kutschera W., Beyerle U., Aeschbach-Herting, Kipfer R., Frape S. K., Herceg A., Moran J., Tolstikhin N. I. and Gröning M., 2003. A comparison of groundwater dating with ^{81}Kr, ^{36}Cl and ^{4}He in four wells of the Great Artesian Basin, Australia, Earth Planet. Sci. Lett. 211, 237-250.

Lehmman B. E. and Purtschert R., 1997. Radioisotope dynamics – the origin and fate of nuclides in groundwater, Appl. Geochem. 12, 727-738.

Lippmann J., Stute M., Torgersen T., Moser D. P., Hall J. A., Lin L., Borcsik M., Bellamy R. E. S., Onstott T. C., 2003. Dating ultra-deep mine waters with noble gases and ^{36}Cl, Witwatersrand Basin, South Africa, Geochim. Cosmochim. Acta. 67, 4597-4619.

Louvant D., Michelot L. J., Aranyossy F. J., 1999. Origin and residence time of salinity in the Äspö groundwater system, Appl. Geochem. 14, 917-925.

Mahara Y., Igarashi T., Hasegawa T., Miyakawa Y., Tanaka Y. and Kiho K, 2001. Dynamic changes in hydrogeochemical condition caused by tunnel excavation at the Äspö Hard Rock Laboratory (HRL), Sweden, Appl. Geochem. 16, 291-315.

Mahara Y. and Igarashi T., 2003. Changes in isotope ratio and content of dissolved helium though groundwater evolution, Appl. Geochim. 18, 719-738.

Mahara Y., Ito Y., Nakamura T. and Kudo A., 2004. Comparison of ^{36}Cl measurements at three laboratories around the world, Nucl. Instr. and Meth. in Phys. Res. B. 223-224, 479-482.

Marine I. W., 1979. The use of naturally occurring helium to estimate groundwater velocities for studies of geologic storage of radioactive waste, Water Resour. Res. 15, 1130-1136.

Martel D. J., Deák J., Dövenyi P., Horváth F., O'Nions R. K., Oxburgh E. R., Stegena L. and Stue M., 1989. Leakage of helium from the Pannonia basin, Nature 342, 908-912.

Marty B., Torgersen T., Meynier V., O'Nions R. K. and de Marsily G., 1993. Helium isotope fluxes and groundwater ages in the Dogger Aquifer, Paris Basin, Water Resour. Res. 29, 1025-1035.

Moran E. J., Fehn U. and Hanor S. J., 1995. Determination of source ages and migration patterns of brines from the U.S. Gulf Coast basin using ^{129}I, Geochim. Cosmochim. Acta. 59, 5055-5069.

O'Nions R. K. and Oxburgh E. R., 1983. Heat and helium in the earth, Nature 306, 429-431.

Osenbrück K., Lippmann J. and Sonntag C., 1998. Dating very old pore waters in impermeable rocks by noble gas isotopes. Geochim. Cosmochim. Acta. 62, 3041-3045.

Park J., Bethke C. M., Torgersen T. and Johnson T.M., 2002. Transport modeling applied to the interpretation of groundwater ^{36}Cl age, Water Resour. Res. 38, No.5, 10.1029/2001WR000399.

Rauber D., Loosli H. H. and Lehmann B. E., 1991. ^{40}Ar/^{36}Ar Ratios, *In Applied Isotope Hydrology, A Case Study in Northern Switerland,(pp.439) F. J. Pearson Jr., W. Balderer, H. H. Loosli, B. E. Lehmann, A. Matter, Tj. Peters, H. Schmassmann and A. Gautschi (Eds),* Studies in Enviromental Science 43., Lesevier, pp. 288-296.

Sano Y., Wakita H. and Huang C. -W., 1986. He flux in a continental land are estimated from ^{3}He/^{4}He ratio in northern Taiwan. Nature, 323, 55-57.

Sano Y., Takahata N., Mahara Y. and Yasuike S., 1993. Precise measurement of helium isotopes in groundwater, Jour. Sci. Hiroshima Univ., Ser. C, 9, 603-610.

Savoye S., 1998. Origine de la salinité des eaux souterrainesen milieu granitique: identification et caractérisation des sources de chlorure, Th. Doct. en. Sci., Univ. Paris-Sud, Orsay.

Solomon D. K., Hunt A. and Poreda R. J., 1996 Source of radiogenic helium 4 in shallow aquifers: Implications for dating young groundwater, Wat. Resour. Res., 1805-1813.

Stanfors R., Rhen I., Tullborg E.-L., Wikberg P., 1999. Overview of geological and hydrogeological conditions of the Äspö hard rock laboratory site, Appl. Geochem. 14, 819-834.

Stute M., Sonntag C., Deak J. and Schlosser P., 1992. Helium in deep circulating groundwater in the Great Hungarian Plain: flow dynamics and crustal and mantle helium fluxes, Geochim. Cosmochim. Acta 56, 2051-2067.

Tolstikhin I.N., Lehmann B.E., Loosli H.H. and Gautschi A., 1996. Helium and argon isotopes in rocks, minerals and related groundwaters: A case study in Northern Switzerland, Geochim. Cosmochim. Acta 60, 1497-1514.

Torgersen T., 1989. Terrestial helium degassing fluxes and the atmospheric helium budget: Implications with respect to the degassing processes of the continental crust. Chem. Geol. 79, 1-14.

Torgersen T. and Clarke W. B., 1985. Helium accumulation in groundwater, I: An evaluation of sources and the continental flux of crustal ^{4}He in the Great Artesian Basin,

Australia, Geochim. Cosmochim. Acta 49, 1211-1218.

Weiss R. F., 1971. Solubility of helium and neon in water and seawater, J. Chem. Eng. Data, 16, 235-241.

Figure Captions

Fig. 1: Location of the Äspö HRL in Sweden and projection of the spiral tunnel (heavy solid line) in the HRL. The open circle indicates the location of the deep borehole Lax-02 at Laxemar.

Fig. 2: (a) Locations of the boreholes for sampling groundwater in the HRL, and the distribution of areas of high groundwater conductivity via fractures. (b) Vertical cross section showing locations and depth of boreholes for sampling groundwater in the tunnel.

Fig. 3: Relationship between dissolved ^{4}He concentration (cm^3STP/m^3) and sampling depth (- z (m)) of groundwater. The fitting curve, which is described by the exponential function given in eq. 1, was drawn using the corrected data for 1995. The measurement error in the ^{4}He concentration was less than 1%.

Fig. 4: Relationship between dissolved ^{4}He concentration and chloride ion concentration in groundwater from 1995 to 2001. Disturbances in the ^{4}He concentration can be seen in all samples of groundwater collected from 1995 to 2001 with more than 200 meq/L of chloride ion concentration. The measurement error in ^{4}He concentration was less than 1%. Squares and solid line, sampled in 1995; open circles and broken line, sampled in 1997; open triangles and dotted line, sampled in 1999; open stars and dash-dot line, sampled in 2001.

Fig. 5: The origin of ^{36}Cl in the Äspö groundwater, as deduced from the relationship between chloride concentration and ^{36}Cl/Cl ratio. The solid squares with error bars

represent Äspö groundwater, modern Baltic seawater, Japan Sea ocean water, commercial mineral waters (European: S. Pellegrino, Thonon, Volvic; Japanese: Tennen Meisui, Shikotsuko Hisui, Tanigawarennpou Meisui, Rokkou Oishii Mizu, Fuji Mineral Water, Sennin Hisui (Mahara et al., 2003)), and brine at Laxemar; the two dash-dot lines represent mixing between commercial mineral waters and ocean water ($^{36}Cl/Cl = 1 \times 10^{-12}/Cl^- + 2.4 \times 10^{-16}$), and mixing between commercial mineral waters and modern Baltic seawater ($^{36}Cl/Cl = 9.85 \times 10^{-13}/Cl^- + 1.53 \times 10^{-15}$); the fine solid circle indicates the brackish and high-saline water in the Äspö groundwater groups.

Fig. 6: Relationship between the $^{36}Cl/Cl$ ratio and the number of ^{36}Cl atoms per liter of water for the Äspö groundwater and brine from the deep borehole Lax-02 at Laxemar. The three dashed lines show the relationship for chloride concentrations of 1000, 5000, and 8000 mg/L. The shaded area indicates where the water is at secular equilibrium with respect to the $^{36}Cl/Cl$ ratio. Field A, enclosed by the dash-dotted line within the shaded area, indicates samples at secular equilibrium at the Äspö site. The solid circles with error bars are brine water measured in this study and by Louvant et al. (1999).

Fig. 7: Mixing lines between present-day Baltic seawater and seven different levels of saline water with different $^{36}Cl/Cl$ ratios and lacking tritium. Present-day Baltic seawater (Cl^-, 3760 mg/L; $^{36}Cl/Cl$, 1×10^{-15}; ^3H, 42 TU in 1992) is shown by the solid circle. Seven different saline waters with respective Cl^- concentrations and $^{36}Cl/Cl$ ratios of (47000 mg/L and 5.05×10^{-14}), (16000 mg/L and 5.05×10^{-14}), (10000 mg/L and 5.05×10^{-14}), (5000 mg/L and 5.05×10^{-14}), (1000 mg/L and 5.05×10^{-14}), (100 mg/L and 1×10^{-13}), and (10 mg/L and 1×10^{-13}) are indicated by the seven solid lines. The thick dash-dotted line

indicates the predicted detection limit (0.3 TU) of tritium in a mixture consisting of modern Baltic seawater (equivalent to 1.14% seawater) in 2001. The five fine dash-dotted lines represent mixtures with 5%, 10%, 25%, 50%, and 75%, respectively, of modern Baltic seawater. Open circles represent groundwater samples with detectable tritium; solid squares, groundwater samples lacking tritium.

Fig. 8: Mixing lines between ancient Baltic seawater and five saline waters with different $^{36}Cl/Cl$ ratios and plots of groundwater samples lacking tritium (solid squares). Ancient Baltic seawater (solid hexagon) had a Cl^- concentration of 8300 mg/L and a $^{36}Cl/Cl$ ratio of 1×10^{-15}. The five saline waters (broken lines) had respective Cl^- concentrations and $^{36}Cl/Cl$ ratios of (47000 mg/L and 5.05×10^{-14}), (16000 mg/L and 5.05×10^{-14}), (10000 mg/L and 5.05×10^{-14}), (5000 mg/L and 5.05×10^{-14}), and 1000 mg/L and 5.05×10^{-14}.

Fig. 9: Relationship between $^{36}Cl/Cl$ ratio and dissolved ^{4}He concentration in groundwater, and the theoretical range of secular equilibrium with respect to the $^{36}Cl/Cl$ ratio in rock at the Äspö site. The shaded area is the secular equilibrium range for the $^{36}Cl/Cl$ ratio in rock. Squares with error bars represent groundwater sampled in 1995; circles with error bars, sampled in 1997; triangles with error bars, sampled in 1999; stars with error bars, sampled in 2001.

Fig. 10: Relationship between groundwater samples at secular equilibrium with respect to the $^{36}Cl/Cl$ ratio and the theoretical growth curves of ^{36}Cl activated in the terrestrial water in rock for the neutron flux intensity at the Äspö site. The data set are fitted with the solid

line, ($\frac{^{36}Cl}{Cl} = 5.26 \times 10^{-14} \cdot (1 - \exp(-126 \times He))$ $r^2 = 0.96$). Squares with error bars represent groundwater samples at secular equilibrium for ^{36}Cl/Cl ratio and lacking tritium; triangle with error bar, present-day Baltic seawater, the starting point of the activation curve.

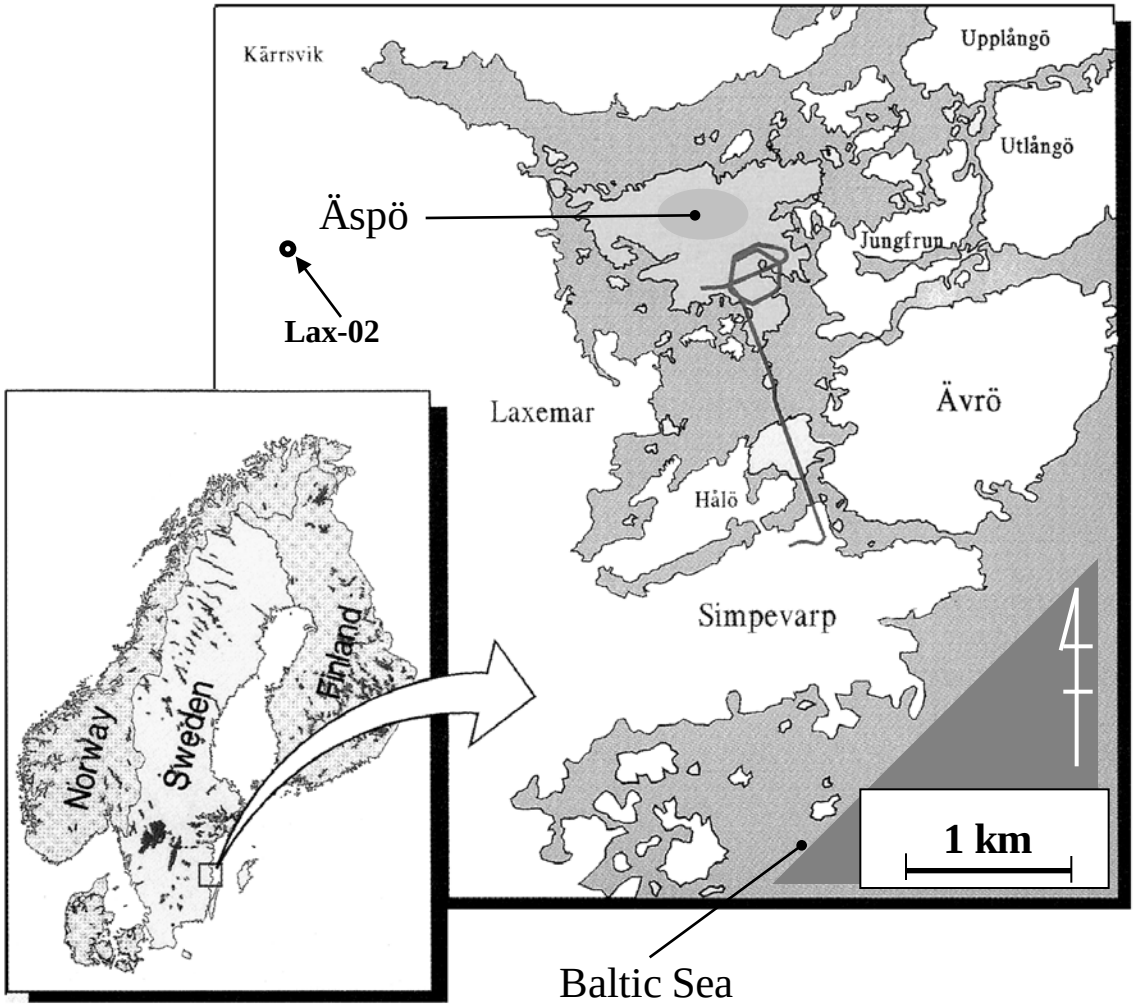
Kärrsvik
Upplångö
Utlångö
Äspö
Jungfrun
Lax-02
Laxemar
Ävrö
Hålö
Simpevarp
1 km
Baltic Sea
Norway
Sweden
Finland

Fig. 1

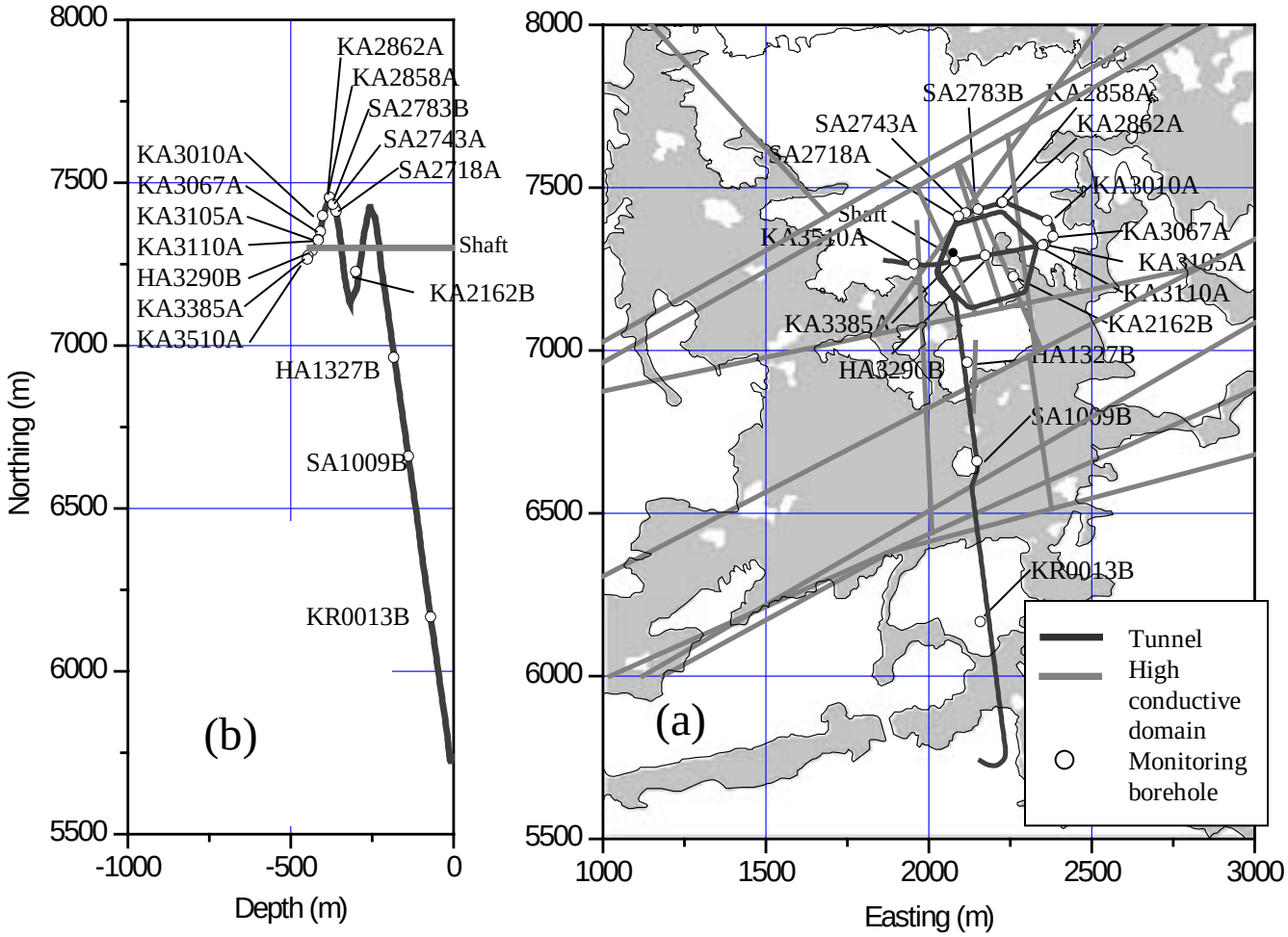
8000
7500
7000
6500
6000
5500
Northing (m)
KA2862A
KA2858A
SA2783B
SA2743A
SA2718A
KA3010A
KA3067A
KA3105A
KA3110A
HA3290B
KA3385A
KA3510A
Shaft
KA2162B
HA1327B
SA1009B
KR0013B
(b)
-1000
-500
0
Depth (m)
1000
1500
2000
2500
3000
Easting (m)
KA3067A
KA3105A
KA3110A
KA2162B
HA1327B
SA1009B
KR0013B
(a)
Tunnel
High conductive domain
Monitoring borehole

Fig. 2

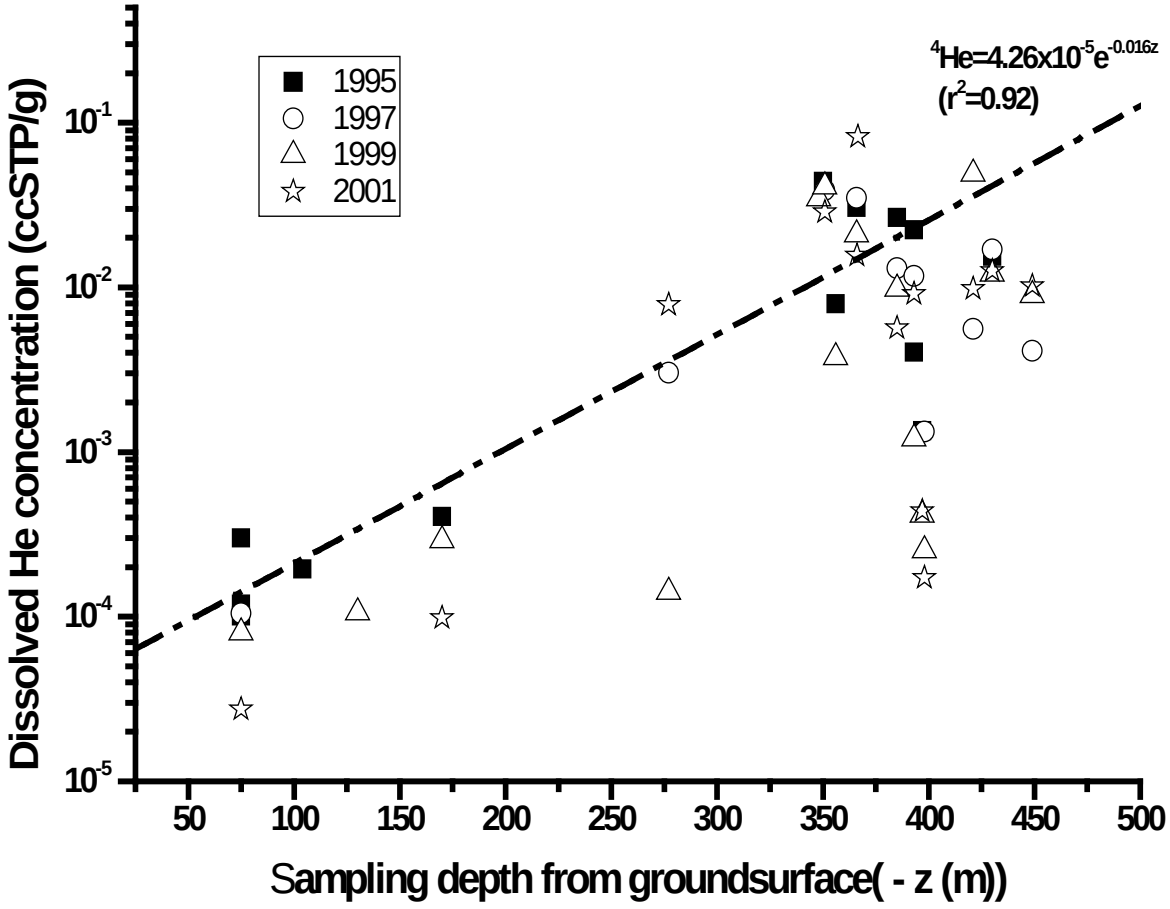
1995
1997
1999
2001
$^4He=4.26x10^{-5}e^{-0.016z}$
(r^2=0.92)
Dissolved He concentration (ccSTP/g)
10^{-1}
10^{-2}
10^{-3}
10^{-4}
10^{-5}
50
100
150
200
250
300
350
400
450
500
Sampling depth from groundsurface(- z (m))

Fig. 3

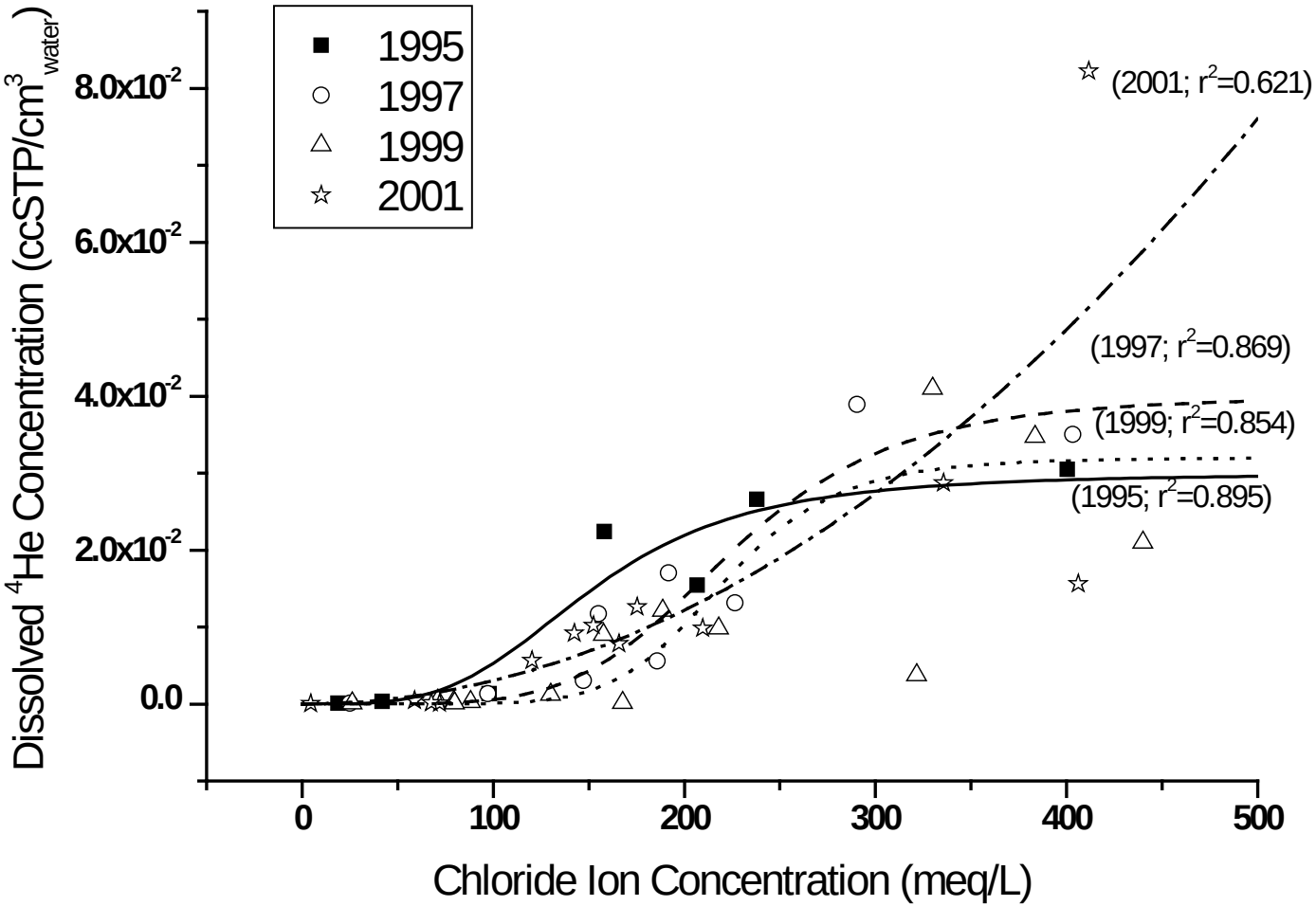
1995
1997
1999
2001
(2001; r2=0.621)
(1997; r2=0.869)
(1999; r2=0.854)
(1995; r2=0.895)
Dissolved 4He Concentration (ccSTP/cm3water)
8.0x10-2
6.0x10-2
4.0x10-2
2.0x10-2
0.0
0
100
200
300
400
500
Chloride Ion Concentration (meq/L)

Fig. 4

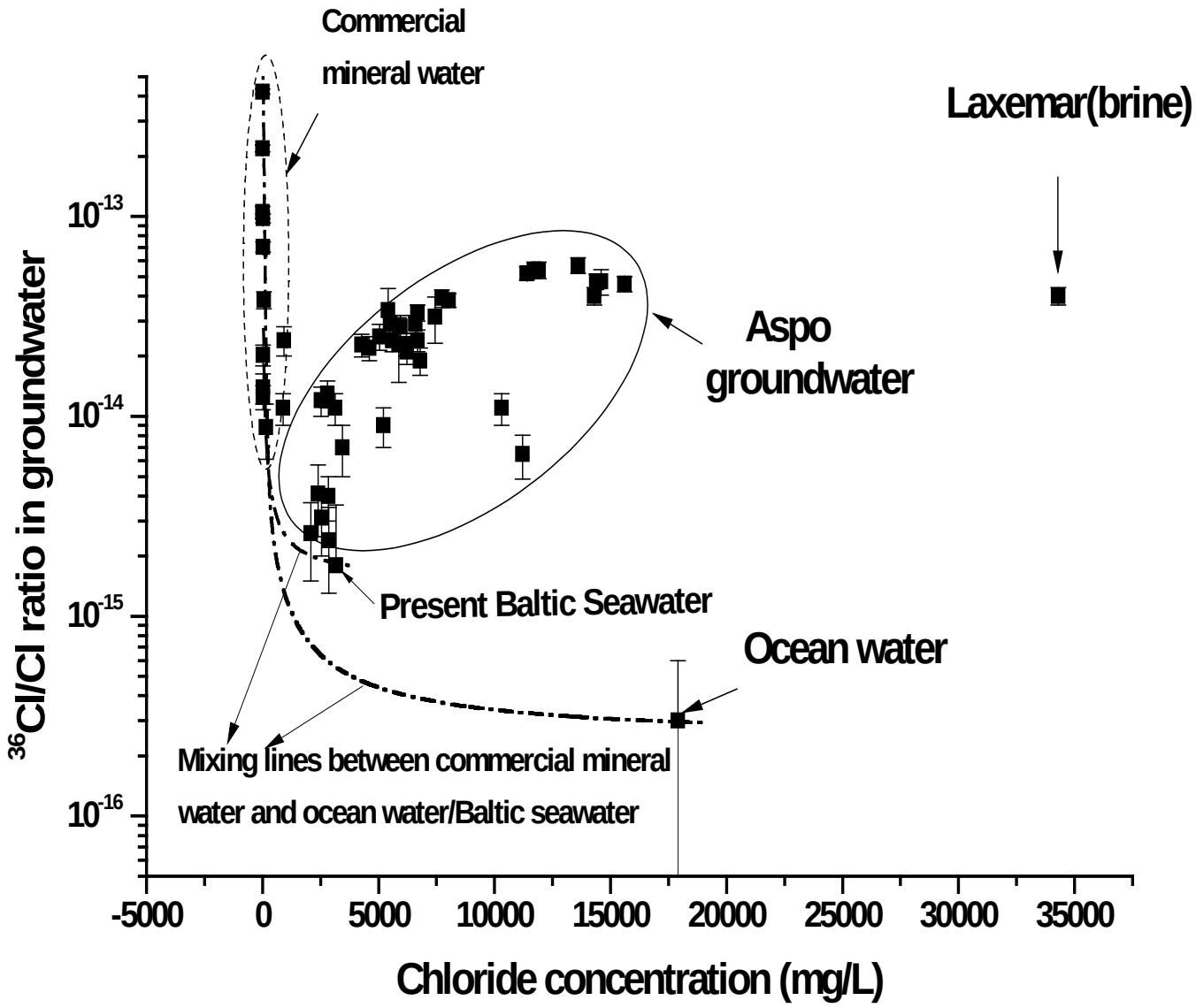
Commercial
mineral water
Laxemar(brine)
Aspo
groundwater
Present Baltic Seawater
Ocean water
Mixing lines between commercial mineral
water and ocean water/Baltic seawater
36Cl/Cl ratio in groundwater
10-13
10-14
10-15
10-16
-5000
0
5000
10000
15000
20000
25000
30000
35000
Chloride concentration (mg/L)

Fig. 5

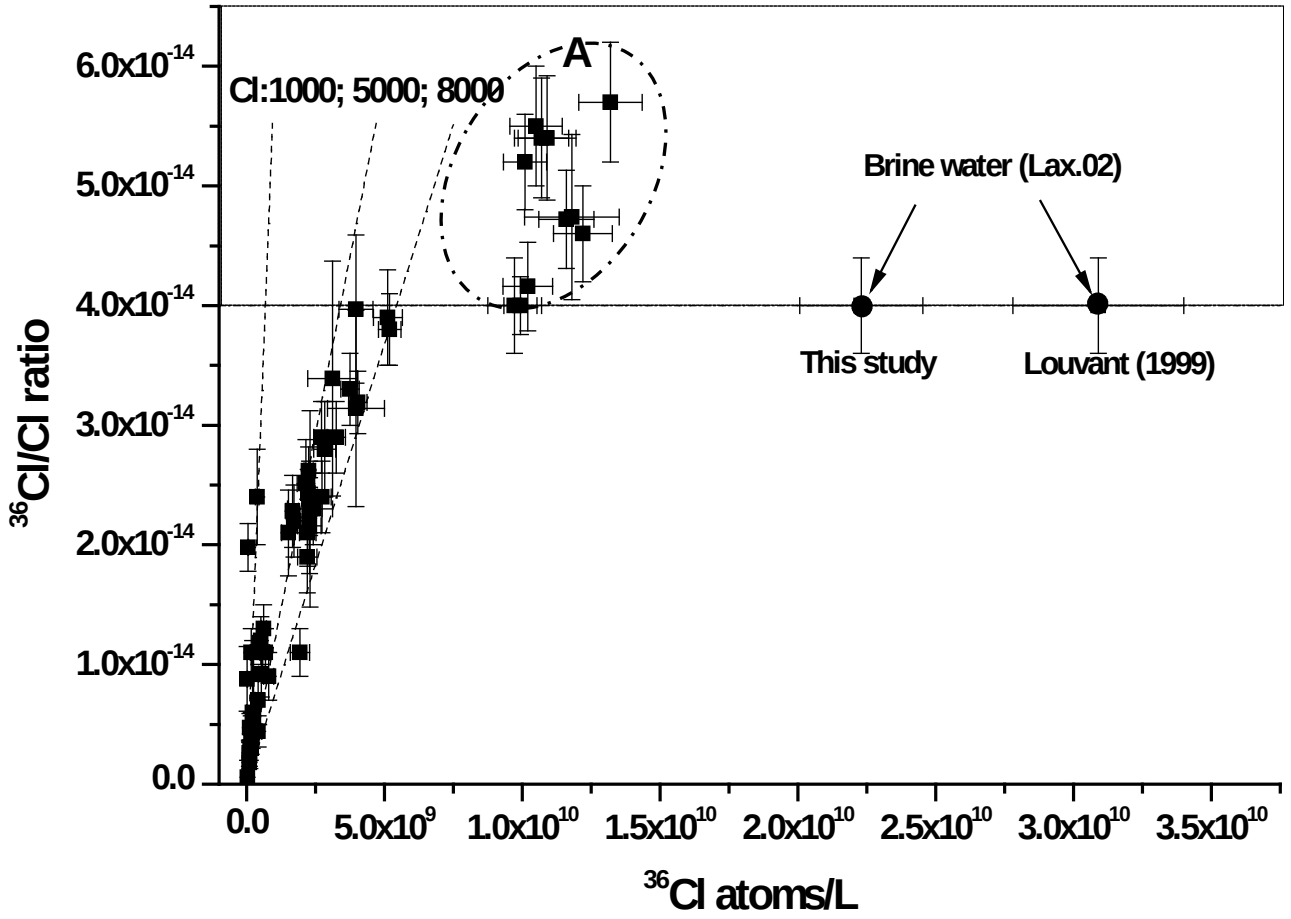
A
Cl:1000; 5000; 8000
Brine water (Lax.02)
This study
Louvant (1999)
^{36}Cl/Cl ratio
^{36}Cl atoms/L
6.0x10^{-14}
5.0x10^{-14}
4.0x10^{-14}
3.0x10^{-14}
2.0x10^{-14}
1.0x10^{-14}
0.0
0.0
5.0x10^{9}
1.0x10^{10}
1.5x10^{10}
2.0x10^{10}
2.5x10^{10}
3.0x10^{10}
3.5x10^{10}

Fig. 6

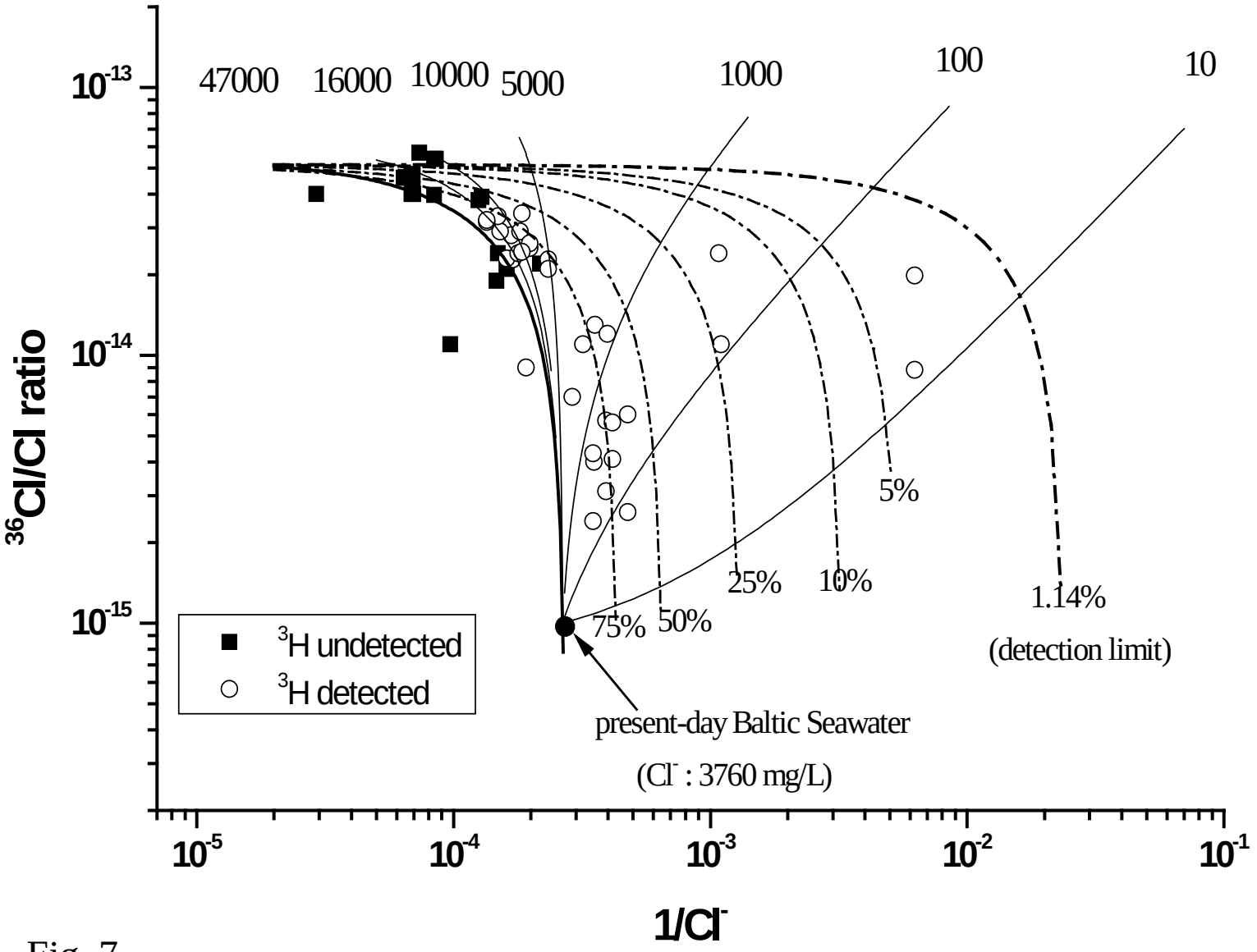
47000
16000
10000
5000
1000
100
10
5%
25%
10%
1.14%
(detection limit)
75%
50%
^{3}H undetected
^{3}H detected
present-day Baltic Seawater
(Cl^{-} : 3760 mg/L)
^{36}Cl/Cl ratio
1/Cl^{-}
10^{-13}
10^{-14}
10^{-15}
10^{-5}
10^{-4}
10^{-3}
10^{-2}
10^{-1}

Fig. 7

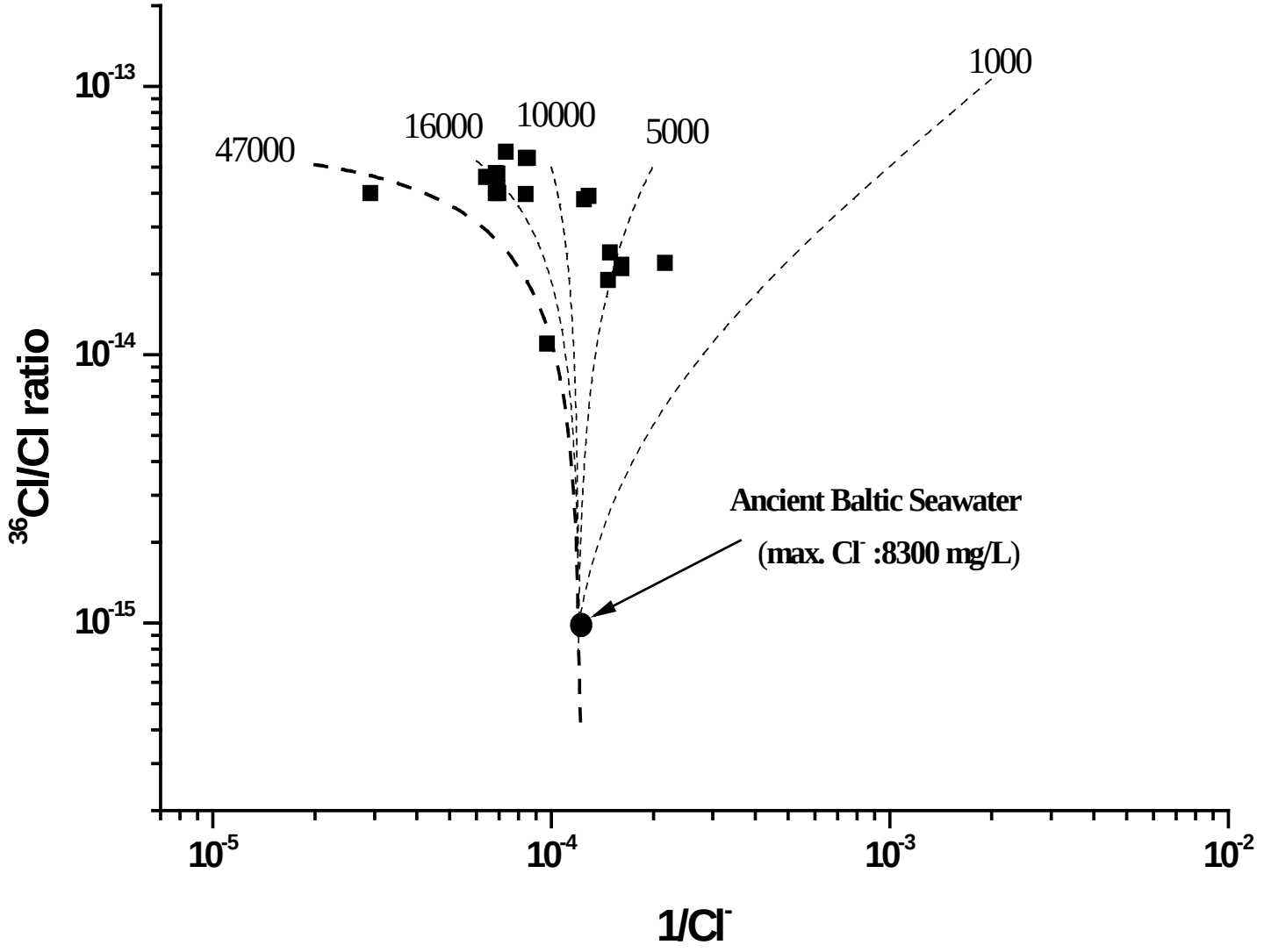
10^{-13}
10^{-14}
10^{-15}
$^{36}Cl/Cl$ ratio
47000
16000
10000
5000
1000
Ancient Baltic Seawater
(max. Cl^- :8300 mg/L)
10^{-5}
10^{-4}
10^{-3}
10^{-2}
$1/Cl^-$

Fig. 8

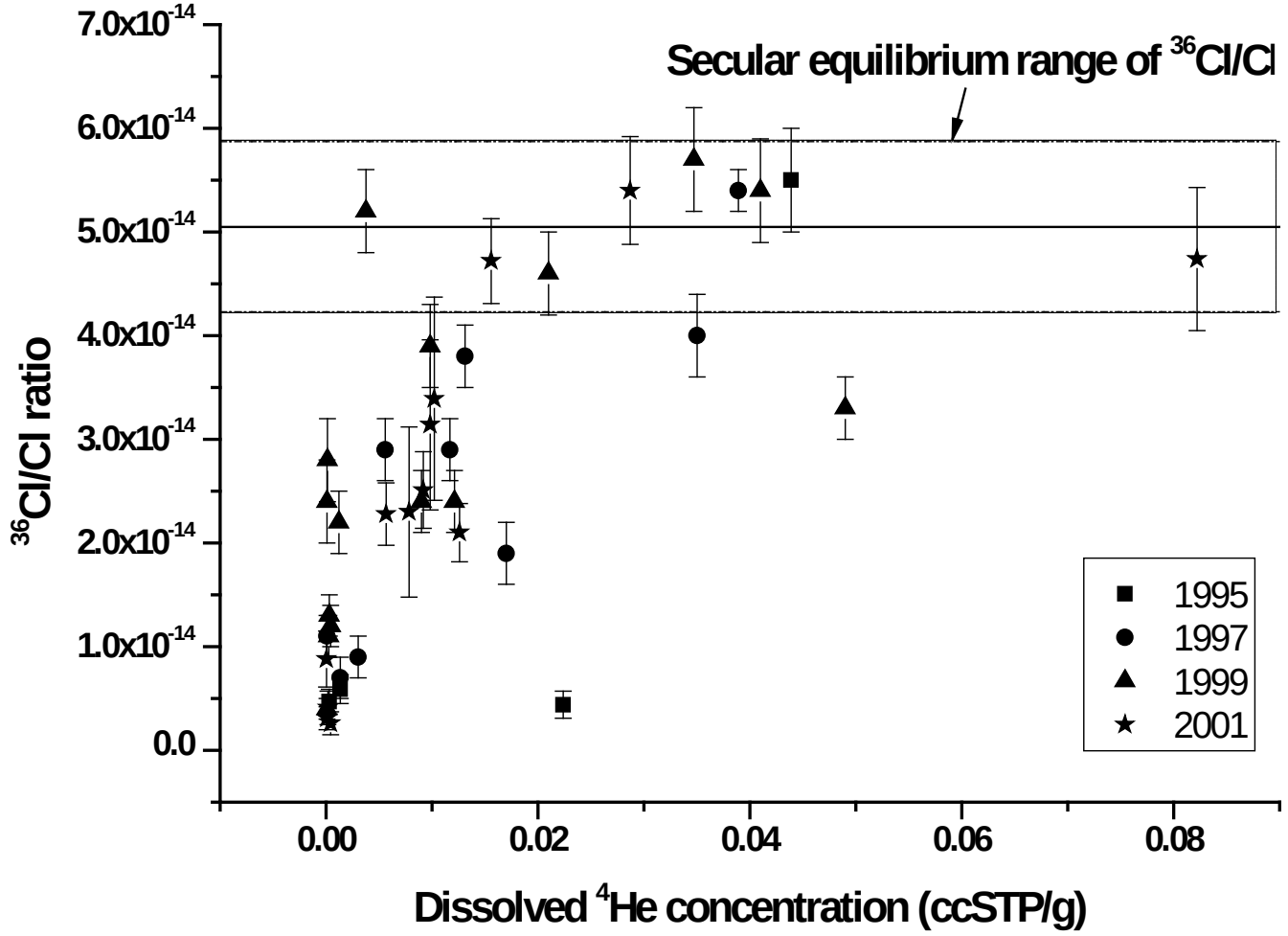
Secular equilibrium range of ^{36}Cl/Cl
^{36}Cl/Cl ratio
7.0x10^{-14}
6.0x10^{-14}
5.0x10^{-14}
4.0x10^{-14}
3.0x10^{-14}
2.0x10^{-14}
1.0x10^{-14}
0.0
0.00
0.02
0.04
0.06
0.08
Dissolved ^{4}He concentration (ccSTP/g)
1995
1997
1999
2001

Fig. 9

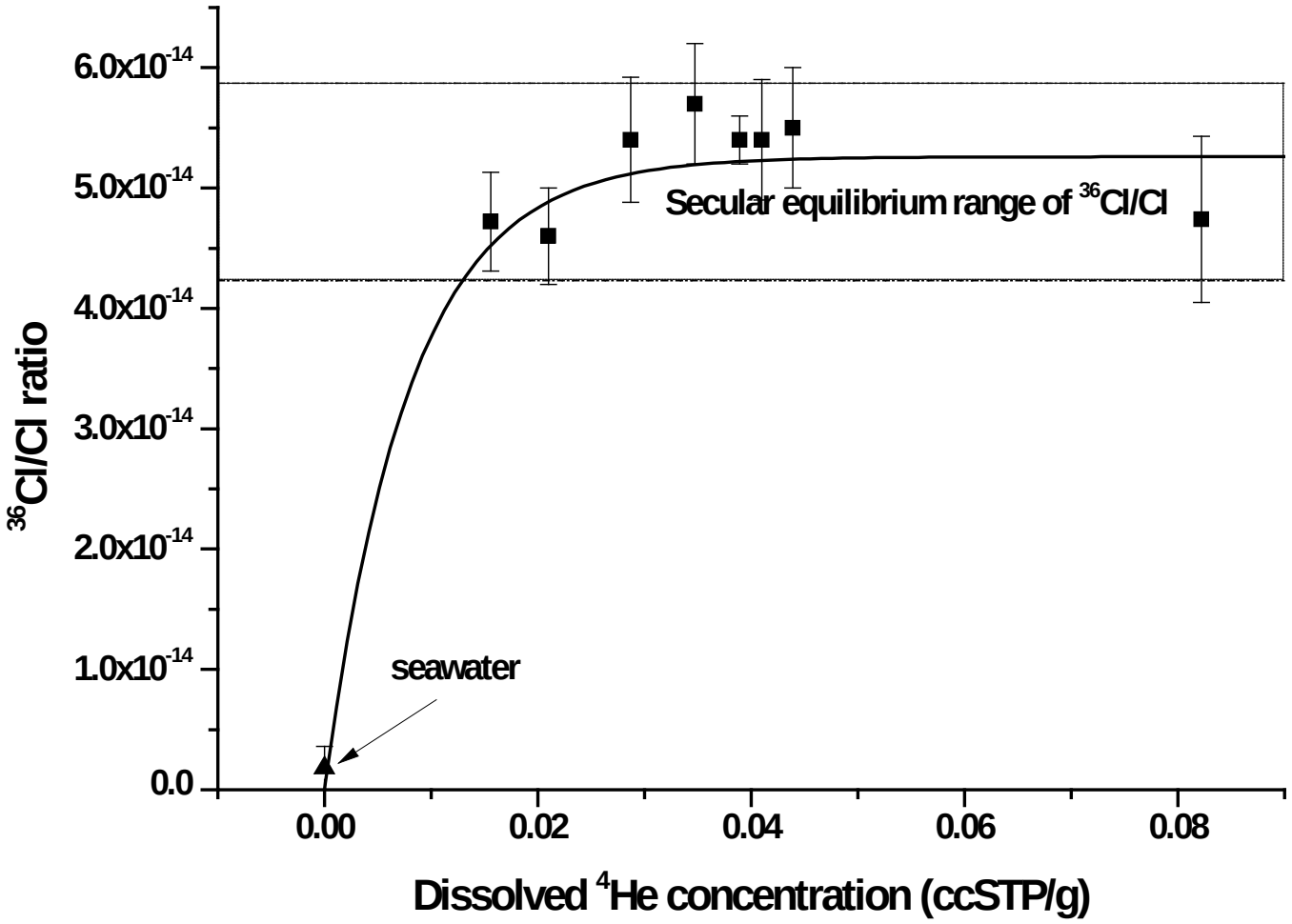
6.0x10-14
5.0x10-14
4.0x10-14
3.0x10-14
2.0x10-14
1.0x10-14
0.0
36Cl/Cl ratio
Secular equilibrium range of 36Cl/Cl
seawater
0.00
0.02
0.04
0.06
0.08
Dissolved 4He concentration (ccSTP/g)

Fig. 10

Table 1. Dissolved noble gases, $^{36}Cl/Cl$, tritium concentration in groundwater at the Äspö site from 1995 to 2001.

Sampling (year)	Date of drilling up	pressure * (Mpa)	^{4}He (ccSTP/g)	$^{3}He/^{4}He$ (mol/mol)	Ne (ccSTP/g)	$^{40}Ar/^{36}Ar$ (mol/mol)	Cl^- (meq/L)	$^{36}Cl/Cl$ (atoms/atoms)	± error (E-15)	^{36}Cl (Atoms/L)	± error	^{3}H (Bq/l)
KR0013B	1991/4/30											
1995		–	3.00E-04	1.15E-08	3.60E-07	3.10E+02	42.018	4.70E-15	±1.2 ‡	1.19E+08	3.04E+07	1.92±0.04
1997		–	1.05E-04	1.90E-08	2.00E-07	2.96E+02	25.0698	1.10E-14	±2	1.66E+08	3.02E+07	1.69±0.03
1999		–	7.79E-05	2.49E-08	1.29E-06	2.97E+02	26.1696	2.40E-14	±4	3.79E+08	6.32E+07	1.87±0.03
2001		–	2.74E-05	1.90E-08	3.29E-07	2.92E+02	4.512	8.80E-15	±2.7	2.39E+07	7.33E+06	1.53±0.03
								1.98E-14	±2 †	5.39E+07	5.44E+06	
HA1327B	1992/9/11											
1995		0.84	4.06E-04	3.04E-08	1.20E-07	2.95E+02	97.572	9.20E-15	±1.9 ‡	5.41E+08	1.12E+08	1.68±0.04
1999		0.65	2.91E-04	1.29E-08	2.90E-06	2.87E+02	79.242	1.30E-14	±2	6.21E+08	9.55E+07	1.72±0.04
2001		0.55	9.81E-05	2.03E-08	3.85E-07	2.75E+02	71.91	3.10E-15	±1.1	1.34E+08	4.75E+07	1.41±0.03
								5.70E-15	±5.7 †	2.47E+08	2.47E+08	
KA2162B	1993/4/1											
1997		2.35	3.02E-03	2.33E-08	8.60E-07	3.20E+02	147.204	9.00E-15	±2	7.99E+08	1.78E+08	0.41±0.02
1999		2.27	1.41E-04	2.25E-08	3.00E-06	3.16E+02	167.79	2.80E-14	±4	2.83E+09	4.04E+08	0.21±0.02
2001		2.2	7.82E-03	1.86E-08	1.23E-06	2.90E+02	165.816	2.30E-14	±8.2	2.30E+09	8.20E+08	0.27±0.02
								2.28E-14	±2 †	2.28E+09	2.00E+08	
SA2743A	Unknown											
1997		–	3.89E-02	2.08E-08	2.30E-05	4.08E+02	290.46	5.40E-14	±2	1.93E+09	3.51E+08	N.D.
1999		–	4.10E-02	2.04E-08	7.02E-07	3.58E+02	329.94	5.40E-14	±5	1.07E+10	9.91E+08	N.D.
2001		–	2.87E-02	2.42E-08	9.28E-06	3.09E+02	335.58	5.40E-14	±5.2	1.09E+10	1.05E+09	N.D.
								3.97E-14	±6.2 †	3.97E+09	6.20E+08	
KA2858A	1995/1/15											
1995		3.6	–	–	–	–	335.58	–		–		N.D.
2001		3.42	1.56E-02	1.63E-08	1.56E-06	3.10E+02	406.08	4.72E-14	±4.1	1.16E+10	1.01E+09	
								4.16E-14	±3.7 †	1.02E+10	9.07E+08	
KA2862A	1995/1/25											
1995		3.58	3.05E-02	1.49E-08	1.00E-06	4.50E+02	400.44	–		–		N.D.
1997		3.35	3.50E-02	2.07E-08	2.80E-07	4.23E+02	403.26	4.00E-14	±4	9.72E+09	9.72E+08	N.D.
1999		3.33	2.10E-02	2.13E-08	5.43E-07	3.97E+02	439.92	4.60E-14	±4	1.22E+10	1.06E+09	N.D.
2001		3.31	8.22E-02	3.23E-08	1.71E-06	3.56E+02	411.72	4.74E-14	±6.9	1.18E+10	1.72E+09	N.D.
								4.00E-14	±2.4 †	9.93E+09	5.96E+08	
KA3010A	1994/12/8											
1995		3.7	2.66E-02	1.09E-08	5.80E-07	3.60E+02	238.008	–		–		N.D.
1997		3.6	1.31E-02	3.48E-08	4.90E-06	3.55E+02	226.446	3.80E-14	±3	5.19E+09	4.10E+08	N.D.
1999		3.59	9.81E-03	4.69E-08	5.64E-07	3.49E+02	217.986	3.90E-14	±4	5.12E+09	5.25E+08	N.D.
2001		3.62	5.65E-03	1.88E-08	6.89E-07	3.07E+02	120.414	2.28E-14	±3.0	1.66E+09	2.18E+08	1.00±0.04
								2.10E-14	±3.6 †	1.52E+09	2.61E+08	
KA3067A	1994/12/11											
1995		3.84	2.24E-02	3.15E-08	4.40E-05	3.03E+02	158.202	4.40E-15	±1.3 ‡	4.20E+08	1.24E+08	0.16±0.04
1997		3.77	1.17E-02	2.42E-08	1.20E-05	3.23E+02	155.1	2.90E-14	±3	2.71E+09	2.80E+08	0.12±0.02
1999		3.76	1.21E-03	8.00E-08	2.62E-07	2.98E+02	130.002	2.20E-14	±3	1.72E+09	2.35E+08	N.D.
2001		3.76	9.16E-03	1.85E-08	4.62E-06	3.04E+02	142.41	2.51E-14	±3.7	2.15E+09	3.17E+08	0.49±0.03
								2.62E-14	±2 †	2.25E+09	1.72E+08	
KA3105A	1994/12/15											
1995		3.8	1.35E-03	1.57E-08	7.50E-08	2.96E+02	97.854	5.90E-15	±1.4 ‡	3.48E+07	8.26E+07	1.00±0.04
1999		3.7	4.17E-04	1.52E-08	2.99E-07	2.86E+02	71.064	1.20E-14	±2	5.14E+08	8.57E+07	1.23±0.03
2001		3.7	4.39E-04	2.37E-08	7.81E-07	3.02E+02	58.938	2.60E-15	±1.1	9.24E+07	3.91E+07	1.49±0.04
								6.00E-15	±6 †	2.13E+08	2.13E+08	
KA3110A	1994/12/17											
1995		3.65	1.32E-03	1.65E-08	1.80E-07	3.03E+02	104.058	1.10E-14	±2.0 ‡	6.90E+08	1.25E+08	1.47±0.04
1997		3.52	1.33E-03	1.89E-08	6.30E-07	2.86E+02	97.29	7.00E-15	±2	4.11E+08	1.17E+08	1.48±0.03
1999		3.45	2.53E-04	1.83E-08	2.99E-07	2.97E+02	88.266	1.10E-14	±2	5.85E+08	1.06E+08	1.56±0.03
2001		3.45	1.72E-04	1.41E-08	4.56E-07	2.90E+02	67.68	4.10E-15	±1.6	1.67E+08	6.52E+07	1.79±0.04
								5.60E-15	±5.6 †	2.28E+08	2.28E+08	
HA3290B	Unknown											
1997		–	5.58E-03	1.70E-08	1.80E-06	3.35E+02	185.838	2.90E-14	±3	3.25E+09	3.36E+08	0.50±0.02
1999		–	4.90E-02	2.09E-08	4.74E-07	3.12E+02	188.658	3.30E-14	±3	3.75E+09	3.41E+08	0.40±0.02
2001		–	9.81E-03	2.11E-08	1.49E-06	3.16E+02	209.526	3.14E-14	±8.2	3.97E+09	1.04E+09	0.16±0.03
								3.19E-14	±2.6 †	4.03E+09	3.28E+08	
KA3385A	1995/1/10											
1995		–	1.54E-02	1.90E-08	2.20E-07	3.47E+02	206.706	–				0.16±0.04
1997		3.81	1.70E-02	2.03E-08	6.60E-06	3.37E+02	191.76	1.90E-14	±3	2.20E+09	3.47E+08	N.D.
1999		3.66	1.21E-02	2.00E-08	4.68E-07	3.23E+02	188.658	2.40E-14	±3	2.73E+09	3.41E+08	N.D.
2001		3.66	1.26E-02	1.86E-08	7.92E-06	3.07E+02	175.404	2.10E-14	±2.8	2.22E+09	2.96E+08	0.07±0.03
								2.16E-14	±4 †	2.28E+09	4.22E+08	
KA3510A	1996/9/9											
1997		–	4.12E-03	2.21E-08	7.40E-08	3.26E+02	174.84	2.30E-14	±3	2.42E+09	3.16E+08	0.25±0.02
1999		4.1	8.99E-03	2.00E-08	3.00E-07	3.02E+02	157.638	2.40E-14	±3	2.28E+09	2.85E+08	0.2±0.02
2001		4.1	1.02E-02	1.85E-08	1.07E-05	2.94E+02	152.562	3.39E-14	±9.8	3.12E+09	9.02E+08	0.22±0.03
								2.43E-14	±2 †	2.23E+09	1.84E+08	
KR0012B	1991/5/3											
1995		–	1.01E-04	4.28E-08	4.20E-06	3.06E+02	18.8658	–		–		1.92±0.04
KR0015B	1991/5/4											
1995		–	1.19E-04	1.65E-08	4.30E-08	2.97E+02	8.7138	–		–		1.91±0.04
SA0813B	Unknown											
1995		–	1.94E-04	1.68E-08	9.20E-08	–	84.318	–		–		1.97±0.04
SA2718A	Unknown											
1995		–	4.39E-02	1.98E-08	1.31E-07	4.27E+02	315.84	5.50E-14	±5 ‡	1.05E+10	9.55E+08	0.09±0.03
1999		–	3.47E-02	2.86E-08	1.17E-05	3.49E+02	383.52	5.70E-14	±5	1.32E+10	1.16E+09	N.D.
SA2783B	Unknown											
1999		–	3.76E-03	2.63E-08	4.18E-06	3.35E+02	321.48	5.20E-14	±4	1.01E+10	7.77E+08	0.20±0.03
SA1009B	Unknown											
1999		–	1.06E-04	1.44E-08	2.68E-06	2.95E+02	79.806	4.00E-15	±1	1.92E+08	4.80E+07	2.00±0.04
2001		–	–	–	–	–	80.652	2.40E-15	±1.1	1.17E+08	5.36E+07	1.52±0.03
								4.30E-15	±4.3 †	2.09E+08	2.09E+08	
Lax-02 (Laxemar) 1999	–	–	1.09E-5 §	2.14E-8 §	1.66E-7 §	292 §	967.26	4.00E-14	±4	3.09E+10	3.09E+09	–
Baltic Seawater 2001	–	–	–	–	–	–	89.394	1.80E-15	±1.8	9.70E+07	9.70E+07	–
								3.00E-15	±3 †	1.62E+08	1.62E+08	

N.D.: Under the detection limit

– : No measurement

*: monitaring static water pressure

†: Analyzed by ETH and other were analyzed by ANU.

‡ : These AgCl precipitated from the residual groundwater samples collected in 1995 were reanalyzed by ANU in 2005.

§: This sample was degased, because groundwater was collected from the water storage tank pumping up from the depth interval of 1420-1705 m of the Lax-02 borehole located at Laxemar.